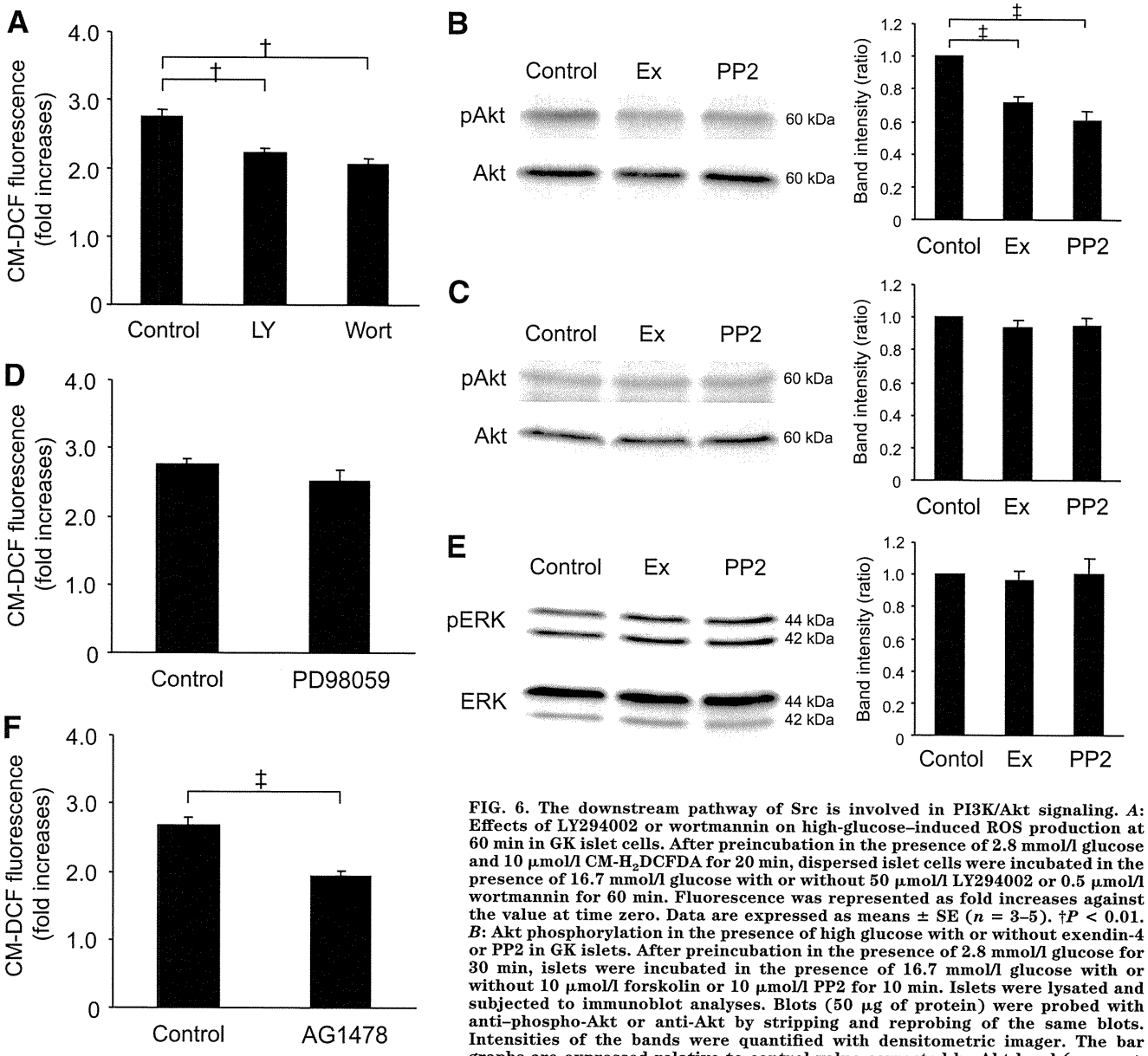

FIG. 6. The downstream pathway of Src is involved in PI3K/Akt signaling. *A*: Effects of LY294002 or wortmannin on high-glucose–induced ROS production at 60 min in GK islet cells. After preincubation in the presence of 2.8 mmol/l glucose and 10 μmol/l CM-H_2DCFDA for 20 min, dispersed islet cells were incubated in the presence of 16.7 mmol/l glucose with or without 50 μmol/l LY294002 or 0.5 μmol/l wortmannin for 60 min. Fluorescence was represented as fold increases against the value at time zero. Data are expressed as means ± SE (n = 3–5). †P < 0.01. *B*: Akt phosphorylation in the presence of high glucose with or without exendin-4 or PP2 in GK islets. After preincubation in the presence of 2.8 mmol/l glucose for 30 min, islets were incubated in the presence of 16.7 mmol/l glucose with or without 10 μmol/l forskolin or 10 μmol/l PP2 for 10 min. Islets were lysated and subjected to immunoblot analyses. Blots (50 μg of protein) were probed with anti–phospho-Akt or anti-Akt by stripping and reprobing of the same blots. Intensities of the bands were quantified with densitometric imager. The bar graphs are expressed relative to control value corrected by Akt level (means ± SE). ‡P < 0.001. Representative blot panels of five independent experiments are shown. *C*: Akt phosphorylation in the presence of high glucose with or without exendin-4 or PP2 in Wistar islets. Representative blot panels of three independent experiments are shown. *D*: Effects of PD98059 on high-glucose–induced ROS production at 60 min in GK islet cells. Data are expressed as means ± SE (n = 4). *E*: ERK phosphorylation in the presence of high glucose with or without exendin-4 or PP2 in GK islets. Blots (50 μg of protein) were probed with anti–phospho-ERK or anti-ERK by stripping and reprobing of the same blots. The bar graphs are expressed relative to control value corrected by ERK level (means ± SE). Representative blot panels of three independent experiments are shown. *F*: Effects of AG1478 on high-glucose–induced ROS production at 60 min in GK islet cells. Data are expressed as means ± SE (n = 5). ‡P < 0.001.

does not affect the phenotype in mice, contrary to neural tube defects and embryonic lethality in homozygous deficient mice (31). Moreover, the localization of Csk in the cytosol before recruitment to the membrane for Src regulation dose not differ in Wistar and GK islets (supplementary Fig. 4). Thus, the lower expression level of Csk found in our results is not likely to play a role in the Src activation in GK islets. Activation of Src as well as elevated endogenous ROS production at high glucose in GK islets was clearly suppressed by exendin-4, which did not affect Src phosphorylation or ROS production in Wistar islets. Thus, the GLP-1 signal might well suppress activation of Src and excessive ROS production under diabetic conditions in addition to other beneficial long-term effects on β-cells.

GLP-1 induces elevation of intracellular cAMP levels and subsequent activation of PKA after binding to the GLP-1 receptor. In the present study, the effect of GLP-1 signaling, which suppresses Src activation and ROS production, was found to be independent of PKA. Epac is a PKA-independent cAMP sensor; Epac2 is expressed mainly in neuroendocrine cells including pancreatic β-cells. Epac2 regulates exocytosis of insulin granules in β-cells by mobilizing intracellular Ca^{2+} and interacting granule-associated proteins (14,15). Although the relationship between Epac and Src is not well known, a recent

report (32) has shown that cAMP protects against hepatocyte apoptosis Epac dependently through Src and PI3K/Akt activation. Further evaluation of the role of cAMP in regulation of Src and PI3K/Akt signaling is required.

In the present study, we have shown that one of these Src signals, the PI3K/Akt signal, regulates ROS production. Furthermore, GLP-1 induces β-cell proliferation through PI3K signaling via Src and EGFR transactivation (33). Our finding that the EGFR kinase inhibitor decreases ROS production suggests that EGFR transactivation may be involved in the ROS-reducing effect of exendin-4 via Src. Under normal conditions, GPCR stimulation generally activates Src toward EGFR transactivation, frequently followed by PI3K activation (25). The present study reveals that Src and PI3K activities are upregulated in islets under diabetic conditions, which are suppressed by the GLP-1 signal. Many studies in oncology have shown that several growth factors including EGF and platelet-derived growth factor induce ROS through PI3K activation (34–36). Thus, EGFR transactivation/PI3K signaling should be activated under pathophysiologically disordered conditions. In the various states between normal and diabetic conditions, the ameliorative effects of the GLP-1 signal may differ (37). Further elucidation of these signals in the pathophysiology of diabetes should be helpful in future development of therapeutic strategies.

Previous studies have shown that the antioxidant capacity in β-cells is very low because of weak expression of antioxidant enzymes in pancreatic islets compared with that in various other tissues (38). The superoxide anion is converted by superoxide dismutase (SOD) into hydrogen peroxide that is eventually removed by glutathione peroxidase (Gpx). The expression level of MnSOD, which is localized in mitochondria, was significantly lower in GK islets than in Wistar islets, and that of of Gpx was similar in Wistar and GK islets (supplementaty Fig. 5*A*). However, an enzymatic assay revealed that MnSOD activity in GK islets was similar to that in Wistar islets and that it was not affected by exendin-4 or PP2 (supplementary Fig. 5*B* and *C*). These results indicate that regulation of MnSOD activity does not play a role in the suppressive effects of ROS production by exendin-4.

One of the important sites of ROS generation in β-cells is the mitochondrial electron transport chain, in which ROS generation increases according to the hyperpolarization of mitochondrial inner membrane derived from accelerated glucose metabolism (39). However, in pathophysiological conditions, NADPH oxidase may play an important role in ROS generation in β-cells. Chronic exposure to proinflammatory cytokines and abundant nutrients including glucose and palmitate augments the expression of a phagocyte-like NADPH oxidase in β-cells (40). Moreover, the expression of NADPH oxidase is increased in islets of diabetic Otsuka Long Evans Tokushima Fatty rats (41). Because Src is involved in regulation of NADPH oxidase activity (42), further examination to elucidate the site of ROS generation related to Src activation in β-cells is needed. On the other hand, previous reports have shown that ROS itself regulates Src activity (43,44) in addition to Src activity regulation of ROS production (45). To clarify this mutual causal relationship between Src and ROS, we examined ROS production in GK islets expressing Src-KN, which was found to cause a distinct decrease in high-glucose–induced ROS production. This finding demonstrates that Src activity regulates ROS production and does not contradict the possibility of a feedback regulation mechanism of ROS on Src activity (45).

The high-glucose–induced increase in ATP production is impaired in GK rats (6,46) as well as in patients with type 2 diabetes (47). In addition, islets in GK rats and human type 2 diabetes are oxidatively stressed (48–50). In the present study, exendin-4 was able to recover this impaired increase in ATP production by high glucose in GK islets as well as to decrease excessive ROS production. Thus, GLP-1 signaling may improve β-cell function in the diabetic state not only because it enhances Ca^{2+} efficacy of the exocytotic system of insulin granules but also because it improves impaired metabolism-secretion coupling. GLP-1 receptor agonists are widely used in treatment of type 2 diabetes for their ability to improve glucose intolerance. Their clinical beneficial effect seems to be provided not only by their insulinotropic action but also by their reduction of β-cell apoptosis and induction of β-cell proliferation (16–18). Further elucidation of endogenous ROS regulation by GLP-1 may help to clarify the mechanism of the various beneficial effects of these agents.

ACKNOWLEDGMENTS

This work was supported by a research grant on Nanotechnical Medicine from the Ministry of Health, Labor, and Welfare of Japan; by scientific research grants from the Ministry of Education, Culture, Sports, Science, and Technology of Japan; and also by the Kyoto University Global Center of Excellence Program Center for Frontier Medicine.

No potential conflicts of interest relevant to this article were reported.

E.M. researched data, contributed to the discussion, wrote the manuscript, and reviewed/edited the manuscript. S.F. contributed to the discussion, wrote the manuscript, and reviewed/edited the manuscript. H.S., C.O., R.K., Y.S., M.S., and Y.N. researched data. M.O. contributed to the discussion and reviewed/edited the manuscript. N.I. contributed to the discussion and reviewed/edited the manuscript.

Parts of this study were presented in abstract form at the 70th Scientific Sessions of the American Diabetes Association, Orlando, Florida, 25–29 June 2010.

We acknowledge the editorial assistance of Dalmen Mayer. We thank C. Kotake for excellent technical assistance.

REFERENCES

1. Maechler P, Wollheim CB. Mitochondrial function in normal and diabetic beta-cells. Nature 2001;414:807–812
2. Krippeit-Drews P, Kramer C, Welker S, Lang F, Ammon HP, Drews G. Interference of H2O2 with stimulus-secretion coupling in mouse pancreatic beta-cells. J Physiol 1999;514(Pt 2):471–481
3. Maechler P, Jornot L, Wollheim CB. Hydrogen peroxide alters mitochondrial activation and insulin secretion in pancreatic beta cells. J Biol Chem 1999;274:27905–27913
4. Bindokas VP, Kuznetsov A, Sreenan S, Polonsky KS, Roe MW, Philipson LH. Visualizing superoxide production in normal and diabetic rat islets of Langerhans. J Biol Chem 2003;278:9796–9801
5. Sakai K, Matsumoto K, Nishikawa T, Suefuji M, Nakamaru K, Hirashima Y, Kawashima J, Shirotani T, Ichinose K, Brownlee M, Araki E. Mitochondrial reactive oxygen species reduce insulin secretion by pancreatic beta-cells. Biochem Biophys Res Commun 2003;300:216–222
6. Kominato R, Fujimoto S, Mukai E, Nakamura Y, Nabe K, Shimodahira M, Nishi Y, Funakoshi S, Seino Y, Inagaki N. Src activation generates reactive oxygen species and impairs metabolism-secretion coupling in diabetic Goto-Kakizaki and ouabain-treated rat pancreatic islets. Diabetologia 2008;51:1226–1235
7. Xu W, Harrison SC, Eck MJ. Three-dimensional structure of the tyrosine kinase c-Src. Nature 1997;385:595–602

8. Martin GS. The hunting of the Src. Nat Rev Mol Cell Biol 2001;2:467–475
9. Nada S, Okada M, MacAuley A, Cooper JA, Nakagawa H. Cloning of a complementary DNA for a protein-tyrosine kinase that specifically phosphorylates a negative regulatory site of p60c-src. Nature 1991;351: 69–72
10. Baggio LL, Drucker DJ. Biology of incretins: GLP-1 and GIP. Gastroenterology 2007;132:2131–2157
11. Holst JJ. The physiology of glucagon-like peptide 1. Physiol Rev 2007;87: 1409–1439
12. Seino S, Shibasaki T. PKA-dependent and PKA-independent pathways for cAMP-regulated exocytosis. Physiol Rev 2005;85:1303–1342
13. Roscioni SS, Elzinga CR, Schmidt M. Epac: effectors and biological functions. Naunyn Schmiedebergs Arch Pharmacol 2008;377:345–357
14. Ozaki N, Shibasaki T, Kashima Y, Miki T, Takahashi K, Ueno H, Sunaga Y, Yano H, Matsuura Y, Iwanaga T, Takai Y, Seino S. cAMP-GEFII is a direct target of cAMP in regulated exocytosis. Nat Cell Biol 2000;2:805–811
15. Kang G, Joseph JW, Chepurny OG, Monaco M, Wheeler MB, Bos JL, Schwede F, Genieser HG, Holz GG. Epac-selective cAMP analog 8-pCPT-2′-O-Me-cAMP as a stimulus for Ca2+-induced Ca2+ release and exocytosis in pancreatic beta-cells. J Biol Chem 2003;278:8279–8285
16. Xu G, Stoffers DA, Habener JF, Bonner-Weir S. Exendin-4 stimulates both β-cell replication and neogenesis, resulting in increased β-cell mass and improved glucose tolerance in diabetic rats. Diabetes 1999; 48:2270–2276
17. Farilla L, Hui H, Bertolotto C, Kang E, Bulotta A, Di Mario U, Perfetti R. Glucagon-like peptide-1 promotes islet cell growth and inhibits apoptosis in Zucker diabetic rats. Endocrinology 2002;143:4397–4408
18. Li Y, Hansotia T, Yusta B, Ris F, Halban PA, Drucker DJ. Glucagon-like peptide-1 receptor signaling modulates beta cell apoptosis. J Biol Chem 2003;278:471–478
19. Tsunekawa S, Yamamoto N, Tsukamoto K, Itoh Y, Kaneko Y, Kimura T, Ariyoshi Y, Miura Y, Oiso Y, Niki I. Protection of pancreatic beta-cells by exendin-4 may involve the reduction of endoplasmic reticulum stress; in vivo and in vitro studies. J Endocrinol 2007;193:65–74
20. Cheng Q, Law PK, de Gasparo M, Leung PS. Combination of the dipeptidyl peptidase IV inhibitor LAF237 [(S)-1-[(3-hydroxy-1-adamantyl)ammo]acetyl-2-cyanopyrrolidine] with the angiotensin II type 1 receptor antagonist valsartan [N-(1-oxopentyl)-N-[[2′-(1H-tetrazol-5-yl)-[1,1′-biphenyl]-4-yl]methyl]-L-valine] enhances pancreatic islet morphology and function in a mouse model of type 2 diabetes. J Pharmacol Exp Ther 2008;327:683–691
21. Akagi T, Sasai K, Hanafusa H. Refractory nature of normal human diploid fibroblasts with respect to oncogene-mediated transformation. Proc Natl Acad Sci U S A 2003;100:13567–13572
22. Florio M, Wilson LK, Trager JB, Thorner J, Martin GS. Aberrant protein phosphorylation at tyrosine is responsible for the growth-inhibitory action of pp60v-src expressed in the yeast Saccharomyces cerevisiae. Mol Biol Cell 1994;5:283–296
23. Mukai E, Fujimoto S, Sakurai F, Kawabata K, Yamashita M, Inagaki N, Mizuguchi H. Efficient gene transfer into murine pancreatic islets using adenovirus vectors. J Control Release 2007;119:136–141
24. Daub H, Weiss FU, Wallasch C, Ullrich A. Role of transactivation of the EGF receptor in signalling by G-protein-coupled receptors. Nature 1996; 379:557–560
25. Rozengurt E. Mitogenic signaling pathways induced by G protein-coupled receptors. J Cell Physiol 2007;213:589–602
26. Eguchi S, Iwasaki H, Inagami T, Numaguchi K, Yamakawa T, Motley ED, Owada KM, Marumo F, Hirata Y. Involvement of PYK2 in angiotensin II signaling of vascular smooth muscle cells. Hypertension 1999;33:201–206
27. Gao Y, Tang S, Zhou S, Ware JA. The thromboxane A2 receptor activates mitogen-activated protein kinase via protein kinase C-dependent Gi coupling and Src-dependent phosphorylation of the epidermal growth factor receptor. J Pharmacol Exp Ther 2001;296:426–433
28. Chiu T, Santiskulvong C, Rozengurt E. EGF receptor transactivation mediates ANG II-stimulated mitogenesis in intestinal epithelial cells through the PI3-kinase/Akt/mTOR/p70S6K1 signaling pathway. Am J Physiol Gastrointest Liver Physiol 2005;288:G182–G194
29. Harris KF, Shoji I, Cooper EM, Kumar S, Oda H, Howley PM. Ubiquitin-mediated degradation of active Src tyrosine kinase. Proc Natl Acad Sci U S A 1999;96:13738–13743
30. Yokouchi M, Kondo T, Sanjay A, Houghton A, Yoshimura A, Komiya S, Zhang H, Baron R. Src-catalyzed phosphorylation of c-Cbl leads to the interdependent ubiquitination of both proteins. J Biol Chem 2001;276: 35185–35193
31. Nada S, Yagi T, Takeda H, Tokunaga T, Nakagawa H, Ikawa Y, Okada M, Aizawa S. Constitutive activation of Src family kinases in mouse embryos that lack Csk. Cell 1993;73:1125–1135
32. Gates A, Hohenester S, Anwer MS, Webster CR. cAMP-GEF cytoprotection by Src tyrosine kinase activation of phosphoinositide-3-kinase p110 beta/alpha in rat hepatocytes. Am J Physiol Gastrointest Liver Physiol 2009;296: G764–G774
33. Buteau J, Foisy S, Joly E, Prentki M. Glucagon-like peptide 1 induces pancreatic β-cell proliferation via transactivation of the epidermal growth factor receptor. Diabetes 2003;52:124–132
34. Zhu QS, Xia L, Mills GB, Lowell CA, Touw IP, Corey SJ. G-CSF induced reactive oxygen species involves Lyn-PI3-kinase-Akt and contributes to myeloid cell growth. Blood 2006;107:1847–1856
35. Baumer AT, Ten Freyhaus H, Sauer H, Wartenberg M, Kappert K, Schnabel P, Konkol C, Hescheler J, Vantler M, Rosenkranz S. Phosphatidylinositol 3-kinase-dependent membrane recruitment of Rac-1 and p47phox is critical for alpha-platelet-derived growth factor receptor-induced production of reactive oxygen species. J Biol Chem 2008;283:7864–7876
36. Binker MG, Binker-Cosen AA, Richards D, Oliver B, Cosen-Binker LI. EGF promotes invasion by PANC-1 cells through Rac1/ROS-dependent secretion and activation of MMP-2. Biochem Biophys Res Commun 2009;379: 445–450
37. Peyot ML, Gray JP, Lamontagne J, Smith PJ, Holz GG, Madiraju SR, Prentki M, Heart E. Glucagon-like peptide-1 induced signaling and insulin secretion do not drive fuel and energy metabolism in primary rodent pancreatic beta-cells. PLoS One 2009;4:e6221
38. Tiedge M, Lortz S, Drinkgern J, Lenzen S. Relation between antioxidant enzyme gene expression and antioxidative defense status of insulin-producing cells. Diabetes 1997;46:1733–1742
39. Newsholme P, Haber EP, Hirabara SM, Rebelato EL, Procopio J, Morgan D, Oliveira-Emilio HC, Carpinelli AR, Curi R. Diabetes associated cell stress and dysfunction: role of mitochondrial and non-mitochondrial ROS production and activity. J Physiol 2007;583:9–24
40. Morgan D, Oliveira-Emilio HR, Keane D, Hirata AE, Santos da Rocha M, Bordin S, Curi R, Newsholme P, Carpinelli AR. Glucose, palmitate and pro-inflammatory cytokines modulate production and activity of a phagocyte-like NADPH oxidase in rat pancreatic islets and a clonal beta cell line. Diabetologia 2007;50:359–369
41. Nakayama M, Inoguchi T, Sonta T, Maeda Y, Sasaki S, Sawada F, Tsubouchi H, Sonoda N, Kobayashi K, Sumimoto H, Nawata H. Increased expression of NAD(P)H oxidase in islets of animal models of Type 2 diabetes and its improvement by an AT1 receptor antagonist. Biochem Biophys Res Commun 2005;332:927–933
42. Chowdhury AK, Watkins T, Parinandi NL, Saatian B, Kleinberg ME, Usatyuk PV, Natarajan V. Src-mediated tyrosine phosphorylation of p47phox in hyperoxia-induced activation of NADPH oxidase and generation of reactive oxygen species in lung endothelial cells. J Biol Chem 2005;280:20700–20711
43. Giannoni E, Buricchi F, Raugei G, Ramponi G, Chiarugi P. Intracellular reactive oxygen species activate Src tyrosine kinase during cell adhesion and anchorage-dependent cell growth. Mol Cell Biol 2005;25:6391–6403
44. Zhang J, Xing D, Gao X. Low-power laser irradiation activates Src tyrosine kinase through reactive oxygen species-mediated signaling pathway. J Cell Physiol 2008;217:518–528
45. Xie Z, Cai T. Na+-K+-ATPase-mediated signal transduction: from protein interaction to cellular function. Mol Interv 2003;3:157–168
46. Hughes SJ, Faehling M, Thorneley CW, Proks P, Ashcroft FM, Smith PA. Electrophysiological and metabolic characterization of single β-cells and islets from diabetic GK rats. Diabetes 1998;47:73–81
47. Anello M, Lupi R, Spampinato D, Piro S, Masini M, Boggi U, Del Prato S, Rabuazzo AM, Purrello F, Marchetti P. Functional and morphological alterations of mitochondria in pancreatic beta cells from type 2 diabetic patients. Diabetologia 2005;48:282–289
48. Ihara Y, Toyokuni S, Uchida K, Odaka H, Tanaka T, Ikeda H, Hiai H, Seino Y, Yamada Y. Hyperglycemia causes oxidative stress in pancreatic β-cells of GK rats, a model of type 2 diabetes. Diabetes 1999;48:927–932
49. Sakuraba H, Mizukami H, Yagihashi N, Wada R, Hanyu C, Yagihashi S. Reduced beta-cell mass and expression of oxidative stress-related DNA damage in the islet of Japanese Type II diabetic patients. Diabetologia 2002;45:85–96
50. Del Guerra S, Lupi R, Marselli L, Masini M, Bugliani M, Sbrana S, Torri S, Pollera M, Boggi U, Mosca F, Del Prato S, Marchetti P. Functional and molecular defects of pancreatic islets in human type 2 diabetes. Diabetes 2005;54:727–735

Diabetologia (2010) 53:1472–1481
DOI 10.1007/s00125-010-1729-5

ARTICLE

Metformin suppresses hepatic gluconeogenesis and lowers fasting blood glucose levels through reactive nitrogen species in mice

Y. Fujita · M. Hosokawa · S. Fujimoto · E. Mukai · A. Abudukadier · A. Obara · M. Ogura · Y. Nakamura · K. Toyoda · K. Nagashima · Y. Seino · N. Inagaki

Received: 25 January 2010 / Accepted: 24 February 2010 / Published online: 29 March 2010

Abstract
Aims/hypothesis Metformin, the major target of which is liver, is commonly used to treat type 2 diabetes. Although metformin activates AMP-activated protein kinase (AMPK) in hepatocytes, the mechanism of activation is still not well known. To investigate AMPK activation by metformin in liver, we examined the role of reactive nitrogen species (RNS) in suppression of hepatic gluconeogenesis.
Methods To determine RNS, we performed fluorescence examination and immunocytochemical staining in mouse hepatocytes. Since metformin is a mild mitochondrial complex I inhibitor, we compared its effects on suppression of gluconeogenesis, AMPK activation and generation of the RNS peroxynitrite ($ONOO^-$) with those of rotenone, a representative complex I inhibitor. To determine whether endogenous nitric oxide production is required for $ONOO^-$ generation and metformin action, we used mice lacking endothelial nitric oxide synthase (eNOS).
Results Metformin and rotenone significantly decreased gluconeogenesis and increased phosphorylation of AMPK in wild-type mouse hepatocytes. However, unlike rotenone, metformin did not increase the AMP/ATP ratio. It did, however, increase $ONOO^-$ generation, whereas rotenone did not. Exposure of eNOS-deficient hepatocytes to metformin did not suppress gluconeogenesis, activate AMPK or increase $ONOO^-$ generation. Furthermore, metformin lowered fasting blood glucose levels in wild-type diabetic mice, but not in eNOS-deficient diabetic mice.
Conclusions/interpretation Activation of AMPK by metformin is dependent on $ONOO^-$. For metformin action in liver, intra-hepatocellular eNOS is required.

Y. Fujita · M. Hosokawa (✉) · S. Fujimoto · E. Mukai · A. Abudukadier · A. Obara · M. Ogura · Y. Nakamura · K. Toyoda · K. Nagashima · Y. Seino · N. Inagaki
Department of Diabetes and Clinical Nutrition, Graduate School of Medicine, Kyoto University, 54 Shogoin, Kawahara-cho, Sakyo-ku, Kyoto 606-8507, Japan
e-mail: hosokawa@metab.kuhp.kyoto-u.ac.jp

E. Mukai
Japan Association for the Advancement of Medical Equipment, Tokyo, Japan

Y. Seino
Kansai Electric Power Hospital, Osaka, Japan

S. Fujimoto · K. Nagashima · N. Inagaki
CREST of Japan Science and Technology Cooperation (JST), Kyoto, Japan

Keywords AMP · AMP-activated protein kinase · Endothelial nitric oxide synthase · Gluconeogenesis · Metformin · Nitric oxide · Peroxynitrite · Reactive nitrogen species

Abbreviations

AMPK	AMP-activated protein kinase
BAEC	Bovine aortic endothelial cells
DCDHF	2,7-Dihydrodichlorofluorescein
eNOS	Endothelial nitric oxide synthase
L-NAME	N^{ω}-Nitro-L-arginine methyl ester
NOS	Nitric oxide synthase
OCT1	Organic cation transporter 1
$ONOO^-$	Peroxynitrite
RNS	Reactive nitrogen species

Introduction

Metformin is one of the most commonly used oral glucose-lowering drugs for type 2 diabetes and is recommended as a first-line drug in recent treatment guidelines of the American Diabetes Association and European Association for the Study of Diabetes [1, 2]. The main target tissue of metformin is liver and its major effect is to decrease hepatic glucose output, which occurs largely due to the suppression of gluconeogenesis, leading to lower fasting blood glucose levels without insulin stimulation and weight gain [3–5]. In addition, metformin has beneficial effects on cardiovascular function and reduces cardiovascular risk in type 2 diabetes [6].

Although metformin has been used clinically for several decades, the mechanisms by which it exerts its glucose-lowering effects are still unclear [7]. Recent studies have demonstrated that therapeutic effects of metformin are mediated by activation of AMP-activated protein kinase (AMPK), leading to a decrease in gluconeogenesis and an increase of fatty acid oxidation in liver and of glucose uptake in skeletal muscle [8–10]. AMPK is a serine/threonine kinase that acts as an energy sensor and is activated in response to reductions of cellular energy levels and to environmental stress, including hypoxia, ischaemia, exercise, ATP depletion and oxidative stress [11, 12]. Although it has been known that AMPK is activated by an increase in the AMP/ATP ratio, the AMPK-activating mechanism also involves other pathways that are dependent on upstream AMPK kinases, including LKB1 kinase and calmodulin-dependent protein kinase kinase in liver and skeletal muscle, respectively [13]. Previous studies reported that metformin had an inhibitory effect on mitochondrial complex I; and, indeed, an inhibition of mitochondrial complex I has been found to increase the AMP/ATP ratio [7, 14, 15]. AMPK activation by metformin was therefore thought to be also mediated by an increase in the AMP/ATP ratio. However, recent studies have reported that metformin action may be mediated without a notable inhibition of mitochondrial metabolism [10, 16].

Recently, a possible role of peroxynitrite ($ONOO^-$), a reactive nitrogen species (RNS), in the mechanism of AMPK activation has been investigated. RNS comprises nitric oxide and its secondary substrates; $ONOO^-$ is generated from superoxide anions (O_2^-) and nitric oxide [17]. Zou et al. reported that metformin activates AMPK through $ONOO^-$ in bovine aortic endothelial cells (BAEC) [18]. However, it is unclear whether RNS generation by metformin is involved in its suppression of hepatic gluconeogenesis or whether RNS generation affects metformin's pharmacological action in lowering of fasting blood glucose levels.

To clarify the mechanism of AMPK activation in liver, we used mouse hepatocytes to investigate the involvement of the AMP/ATP ratio and RNS in AMPK activation by metformin compared with rotenone, a representative complex I inhibitor. To determine whether endogenous nitric oxide production is required for metformin action in hepatocytes, we also performed experiments using mice lacking endothelial nitric oxide synthase (eNOS) [18–21]. We demonstrated that $ONOO^-$ plays a critical role in AMPK activation by metformin in liver and that eNOS is required for metformin action in vitro and in vivo.

Methods

Animals Male C57/BL6 (wild-type) mice were obtained from Shimizu (Kyoto, Japan). Male eNOS-deficient (*eNos* [also known as *Nos3*]$^{-/-}$) mice were obtained from Jackson Laboratories (Bar Harbor, ME, USA). Mice were maintained in a temperature-controlled (25±2°C) environment with a 12 h light/dark cycle. The mice had free access to standard laboratory chow and water. All experiments were carried out with mice aged 8 to 10 weeks. The animals were maintained and used in accordance with the Guidelines for Animal Experiments of Kyoto University. All the experiments involving animals were conducted in accordance with the Guidelines for Animal Experiments of Kyoto University and were approved by the Animal Research Committee, Graduate School of Medicine, Kyoto University.

Hepatocyte preparation and culture Mice hepatocytes were isolated by collagenase digestion as described previously [22]. Primary hepatocytes were prepared by seeding in six well type 1 collagen-coated plates at a density of 1.5×10^6 cells in DMEM (low glucose, 5.6 mmol/l) containing 10% (vol./vol.) FBS, 100 nmol/l regular insulin, 50 U/ml penicillin and 50 μg/ml streptomycin. Hepatocytes were then cultured overnight in a humidified atmosphere (5% CO_2) at 37°C.

Glucose production via gluconeogenesis in hepatocytes Gluconeogenesis was measured as described previously with slight modifications [22, 23]. In brief, freshly isolated hepatocytes from mice fasted for 16 h were treated in 24 well plates (7.5×10^5 cells/well) in 0.5 ml KRB buffer (119.4 mmol/l NaCl, 3.7 mmol/l KCl, 2.7 mmol/l $CaCl_2$, 1.3 mmol/l KH_2PO_4, 1.3 mmol/l $MgSO_4$, 24.8 mmol/l $NaHCO_3$) containing 2% (wt/vol.) BSA, 2 mmol/l oleate, 0.24 mmol/l 3-isobutyl-1-methylxanthine and gluconeogenetic substrates (1 mmol/l pyruvate plus 10 mmol/l lactate) treated with metformin (Sigma, St Louis, MO, USA) and rotenone (Nacalai Tesque, Kyoto, Japan). Metformin was dissolved in water. Rotenone was dissolved in dimethyl sulfoxide to a concentration that did not interfere with cell viability (maximally 0.1% vol./vol.).

The glucose content of the supernatant fraction was measured by the glucose oxidation method using an assay kit (Gopod; Megazyme, Wicklow, Ireland). The data were normalised by protein content measured by cell lysates.

Immunoblotting analysis Freshly isolated hepatocytes were treated with metformin, rotenone and $ONOO^-$ (Dojindo, Kumamoto, Japan) in KRB buffer containing 2% (wt/vol.) BSA, 2 mmol/l oleate, 0.24 mmol/l 3-isobutyl-1-methylxanthine and gluconeogenetic substrates (1 mmol/l pyruvate plus 10 mmol/l lactate). Primary hepatocytes cultured overnight were incubated in FBS-free DMEM (no glucose) treated with metformin and rotenone. The hepatocytes were homogenised in lysis buffer (50 mmol/l Tris–HCl, pH 7.4, 50 mmol/l NaF, 1 mmol/l sodium pyrophosphate, 1 mmol/l EDTA, 1 mmol/l EGTA, 1 mmol/l dithiothreitol, 0.1 mmol/l benzamidine, 0.1 mmol/l phenylmethylsulfonylfluoride, 0.2 mmol/l sodium vanadate, 250 mmol/l mannitol, 1% (vol./vol.) Triton X-100 and 5 μg/ml soybean trypsin inhibitor). Cell lysates (50 to 150 μg protein per lane) were subjected to electrophoresis on 8% (vol./vol.) SDS–polyacrylamide gels and transferred on to nitrocellulose membranes (Protran; Schleicher and Schuell, Keene, NH, USA). Blotted membranes were incubated with each primary antibody (1:1,000 dilution). Antibodies against AMPKα and phospho-AMPKα (Thr^{172}) were from Cell Signaling Technology (Danvers, MA, USA). Antibodies against organic cation transporter 1 (OCT1) and glyceraldehyde-3-phosphate dehydrogenase were from Santa Cruz Biotechnology (Santa Cruz, CA, USA). Membranes were incubated with horseradish peroxidase-linked second antibodies (1:2,000 dilution) (GE Healthcare, Tokyo, Japan) and fluorescent bands were visualised using a western blotting detection system (Amersham ECL Plus; GE Healthcare) and then quantified by densitometry using Image J software from National Institutes of Health (Bethesda, MD, USA).

Determination of reactive nitrogen species $ONOO^-$ generation was measured using 2,7-dihydrodichlorofluorescein (DCDHF) diacetate (Cayman Chemical, Ann Arbor, MI, USA) [24–26], which is readily oxidised by $ONOO^-$ to the highly fluorescent product, dichlorofluorescein. Alone, nitric oxide, superoxide anions or hydrogen peroxide did not oxidise DCDHF. Freshly isolated hepatocytes were washed in ice-cold PBS and preloaded for 20 min at 37°C with 10 μmol/l DCDHF diacetate (Cayman Chemical) in KRB buffer containing 2% (wt/vol.) BSA, 2 mmol/l oleate, 0.24 mmol/l 3-isobutyl-1-methylxanthine and gluconeogenetic substrates (1 mmol/l pyruvate plus 10 mmol/l lactate). Fluorescence was determined using a spectrofluorophotometer (RF-5300PC; Shimazu, Kyoto, Japan) with excitation wavelength at 502 nm and emission wavelength at 523 nm. After 1 h incubation in the presence or absence of metformin, rotenone, $ONOO^-$ or hydrogen peroxide with or without RNS scavenger (5 mmol/l α-tocopherol plus 2.3 mmol/l ascorbate) [27], fluorescence was measured and presented as a ratio with respect to the value at time zero.

Immunocytochemistry Primary hepatocytes were plated on cover glass coated with 0.01% (vol./vol.) poly-L-lysine (Sigma) in six-well plates (5.0×10^5 cells per well). Hepatocytes were then incubated with FBS-free DMEM (no glucose) in the presence or absence of rotenone, metformin, metformin with RNS scavenger (5 mmol/l α-tocopherol plus 2.3 mmol/l ascorbate) and metformin with 1 mmol/l of the nitric oxide synthase (NOS) inhibitor N^{ω}-nitro-L-arginine methyl ester (L-NAME) for 2 h, or in the presence or absence of $ONOO^-$ for 5 min. The hepatocytes were fixed in 3.7% (wt/vol.) paraformaldehyde and incubated with rabbit polyclonal anti-nitrotyrosine antibody (1:100 dilution; Millipore; Billerica, MA, USA). Next, cells were incubated with goat anti-rabbit IgG fluorescein-conjugated secondary antibody (1:100 dilution; Alexa Fluor 488; Invitrogen, Carlsbad, CA, USA). Fluorescence in cells was monitored using a laser scanning microscope (LSM 510; Carl Zeiss, Tokyo, Japan) for confocal microscopy and a software package (LSM 510 Meta; Carl Zeiss) for image acquisition.

Measurement of adenine nucleotide content After freshly isolated hepatocytes were incubated in KRB buffer containing 2% (wt/vol.) BSA, 2 mmol/l oleate, 0.24 mmol/l 3-isobutyl-1-methylxanthine and gluconeogenetic substrates (1 mmol/l pyruvate plus 10 mmol/l lactate) in the presence or absence of metformin or rotenone for 2 h, or of $ONOO^-$ for 5 min, treatment was stopped by rapid addition of 0.1 ml of 2 mol/l $HClO_4$, followed by mixing by vortex and sonication in ice-cold water for 3 min. Cell lysates were then centrifuged for 3 min at 3,000×*g* and 4°C, and a fraction (0.4 ml) of the supernatant fraction was mixed with 0.1 ml of 2 mol/l HEPES and 0.1 ml of 1 mol/l Na_2CO_3. Adenine nucleotide contents were measured by a luminometric method as previously described [28, 29].

Effect of metformin on plasma glucose levels and AMPK phosphorylation in liver tissue of wild-type and $eNos^{-/-}$ diabetic mice Mice were made diabetic by intraperitoneal injection of streptozotocin (120 mg/kg) into male C57/BL6 and $eNos^{-/-}$ mice at 8 weeks of age. At 1 week after injection of streptozotocin, the animals were confirmed to be diabetic by high fed blood glucose levels (≥13.8 mmol/l) and other diabetic features, including polyuria, polydispia and hyperphagia. After fasting for 16 h, the blood glucose levels were measured and mice were immediately injected intraperitoneally with metformin (250 mg/kg) in 0.9%

sterile saline or 0.9% (wt/vol.) sterile saline only, a similar treatment to that described previously [8, 18]. Blood glucose levels were measured again after 1 h. Diabetic mice received injections of metformin or vehicle as described above for three consecutive days and blood glucose levels were measured again after fasting for 16 h. Immediately after the final measurement of blood glucose levels, the abdomen was cut open and liver tissue of each group was collected and homogenised in lysis buffer. Tissue lysates (50 μg protein/lane) were used for immunoblotting assay of AMPK phosphorylation using antibodies against AMPKα and phospho-AMPKα (Thr^{172}).

Statistical analysis Results are expressed as mean ± SE per number (n) of animals. Statistical significance was evaluated by ANOVA, unpaired t test (not noted) and paired t test (noted). A value of $p<0.05$ was considered statistically significant.

Results

Effects of metformin and rotenone on gluconeogenesis and AMPKα phosphorylation in C57/BL6 mice hepatocytes Hepatic gluconeogenesis and AMPKα phosphorylation were measured using freshly isolated hepatocytes. After 2 h exposure to metformin, hepatic gluconeogenesis was significantly and dose-dependently suppressed at doses between 0.5 and 50 mmol/l metformin; it was also suppressed by exposure to 100 nmol/l rotenone (control 115.4±2.5 nmol/mg protein, 2 mmol/l metformin 92.1±3.3 nmol/mg protein, $p<0.05$ vs control; 100 nmol/l rotenone 91.5±8.7 nmol/mg protein, $p<0.05$ vs control; Fig. 1a). Gluconeogenesis at 2 mmol/l metformin and 100 nmol/l rotenone were similar (p=NS metformin vs rotenone). After 2 h exposure, metformin (0.5–50 mmol/l) and 100 nmol/l rotenone each stimulated phosphorylation of Thr^{172} of AMPKα (Fig. 1b, c). Increments of phosphorylation relative to control in hepatocytes exposed to 2 mmol/l metformin and 100 nmol/l rotenone were almost equivalent (fold increase relative to control 1.79±0.11 [metformin] and 1.85±0.12 [rotenone], p=NS, metformin vs rotenone). Similar results were observed using primary cultured hepatocytes (Fig. 1d, e). In the time course study of exposure to 2 mmol/l metformin, the suppressing effects on gluconeogenesis appeared after 120 min ($p < 0.05$ vs corresponding control; Fig. 1f). In addition, after 60 min exposure to 2 mmol/l metformin stimulated phosphorylation of Thr^{172} of AMPKα ($p<0.05$ vs pre-exposure; Fig. 1g, h).

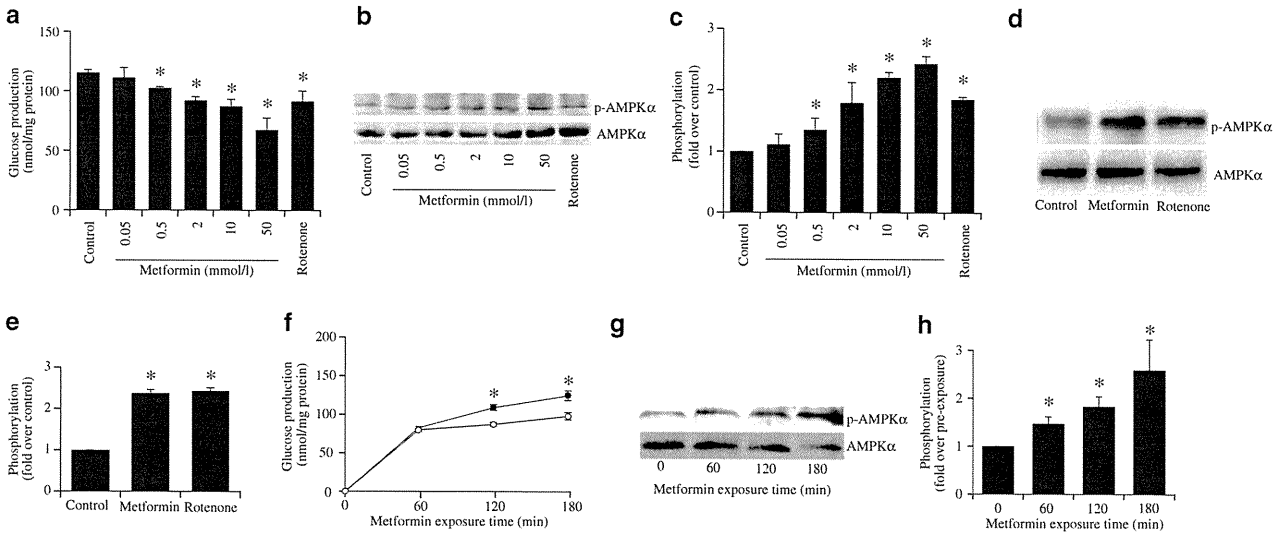

Fig. 1 Metformin and rotenone suppress gluconeogenesis and stimulate AMPKα phosphorylation in hepatocytes isolated from C57/BL6 mice. **a** Gluconeogenesis after 2 h exposure to metformin and rotenone. Metformin (dose-dependently between 0.5 and 50 mmol/l) and rotenone (100 nmol/l) significantly suppressed gluconeogenesis. **b**, **c** Effects of metformin and rotenone on activation of AMPK. After 2 h exposure, AMPKα phosphorylation in freshly isolated hepatocytes was significantly stimulated by metformin (dose-dependently as above [**a**]) and rotenone (100 nmol/l). Data are expressed as fold stimulation over control. **d**, **e** Effects of metformin and rotenone on activation of AMPK in primary cultured hepatocytes. After 2 h exposure, AMPKα phosphorylation was significantly stimulated by metformin (2 mmol/l) and rotenone (100 nmol/l). Data are expressed as fold stimulation over control. **f** Time course of gluconeogenesis with exposure to metformin. Suppressing effects on gluconeogenesis by 2 mmol/l metformin (white circles) compared with control (black circles) were detected after 120 min. **g**, **h** Time course of AMPK activation upon exposure to metformin (2 mmol/l), which after 60 min stimulated phosphorylation of AMPKα in freshly isolated hepatocytes. Data are expressed as fold stimulation over pre-exposure. Values (all bar graphs) are means ± SE (n=6), *$p<0.05$ vs control (**a**–**f**) and pre-exposure (**h**)

ATP content and AMP/ATP ratio in C57/BL6 mice hepatocytes In wild-type mice, exposure of freshly isolated hepatocytes to 100 nmol/l rotenone for 2 h decreased ATP content and increased the AMP/ATP ratio compared with control (Table 1). However, 2 h exposure to 2 mmol/l metformin did not alter ATP content or AMP/ATP ratio compared with control. ATP content and the AMP/ATP ratio at 2 mmol/l metformin and 100 nmol/l rotenone were significantly different ($p<0.01$ metformin vs rotenone).

RNS production by metformin In freshly isolated hepatocytes, exposure to 2 mmol/l metformin for 1 h increased DCDHF fluorescence, revealing an increase of $ONOO^-$ generation, whereas 300 μmol/l hydrogen peroxide or 100 nmol/l rotenone had no effect on DCDHF fluorescence (Table 2). Co-administration of RNS scavengers (vitamin E plus vitamin C) completely suppressed RNS production by metformin.

Immunocytochemical staining of primary cultured hepatocytes with anti-nitrotyrosine antibody was performed to detect $ONOO^-$ (Fig. 2). $ONOO^-$ (10 μmol/l) incubated for 5 min in primary hepatocytes increased nitrotyrosine staining. Exposure to 2 mmol/l metformin, but not to 100 nmol/l rotenone for 2 h increased nitrotyrosine staining (Fig. 2a). Similarly to the DCDHF fluorescence study, co-administration of RNS scavengers (vitamin E plus vitamin C) suppressed nitrotyrosine staining by metformin. Co-administration of L-NAME, a NOS inhibitor, suppressed $ONOO^-$ generation by metformin (Fig. 2b).

Effect of direct exposure to $ONOO^-$ on AMPKα phosphorylation and AMP/ATP ratio The direct effect of exogenous $ONOO^-$ on AMPK phosphorylation in the absence of metformin was examined. Exposure to $ONOO^-$ for 5 min stimulated phosphorylation of AMPKα by 1 to 100 μmol/l ($p < 0.05$ vs control) (Fig. 3a, b). Exposure to 10 μmol/l $ONOO^-$ for 5 min did not affect ATP content (pre-exposure 0.49±0.05 nmol/mg protein; 5 min $ONOO^-$ 0.50±0.05 nmol/mg protein, p = NS vs pre-exposure, n=5) or the AMP/ATP ratio (pre-exposure 0.99±0.06, 5 min $ONOO^-$ 0.98±0.05, p = NS vs pre-exposure, n=5).

Table 1 Effect of metformin or rotenone on ATP content and AMP/ATP ratio in hepatocytes

Treatments per mouse type	ATP (nmol/mg protein)	AMP/ATP ratio
Wild-type mice		
Control	0.45±0.08	0.98±0.07
Metformin	0.47±0.05	0.96±0.12
Rotenone	0.13±0.02**	1.94±0.13**
eNos$^{-/-}$ mice		
Control	0.42±0.07	1.22±0.11
Metformin	0.41±0.06	1.27±0.16
Rotenone	0.11±0.03**	2.34±0.23**

Values are means ± SE (n=5)

**$p<0.01$ vs control

No effect of metformin on gluconeogenesis, AMPKα phosphorylation or $ONOO^-$ generation in hepatocytes lacking eNOS In freshly isolated hepatocytes from *eNos*$^{-/-}$ mice, 2 h exposure to 2 mmol/l metformin did not suppress gluconeogenesis, whereas exposure to 100 nmol/l rotenone suppressed gluconeogenesis to a similar degree to that observed in wild-type hepatocytes (control 110.1± 4.4 nmol/mg protein, metformin 107.0±3.9 nmol/mg protein, p=NS vs control; rotenone 81.6±8.8 nmol/mg protein, $p<0.05$ vs control; Fig. 4a). Metformin did not stimulate AMPKα phosphorylation in freshly isolated hepatocytes from *eNos*$^{-/-}$ mice, whereas rotenone significantly stimulated AMPKα phosphorylation (fold increase relative to control at 2 h: metformin 0.96±0.12, p=NS vs control; rotenone 1.94±0.13, $p<0.05$ vs control; Fig. 4b, c). Similarly, in primary cultured hepatocytes, metformin also did not stimulate, whereas rotenone significantly stimulated AMPKα phosphorylation (Fig. 4d, e). Metformin also did not increase nitrotyrosine staining in primary cultured hepatocytes from *eNos*$^{-/-}$ mice, indicating no generation of $ONOO^-$ (Fig. 4f). In addition, nitrotyrosine staining was not induced by 2 h exposure to rotenone. Exposure of *eNos*$^{-/-}$ freshly isolated hepatocytes to 100 nmol/l rotenone also decreased ATP content and increased the AMP/ATP ratio, whereas exposure to metformin had not effect (Table 1). Recently, it was reported that metformin is first transported across the plasma membrane before exerting its cellular action, a step mediated by OCT1 [30]. To exclude involvement of OCT1 in *eNos*$^{-/-}$ mice, we confirmed that levels of OCT1 protein in freshly isolated hepatocytes from *eNos*$^{-/-}$ mice were similar to those in wild-type mice hepatocytes (Fig. 4g).

Essential role of eNOS in lowering of glucose levels by metformin in diabetic mice in vivo To determine whether metformin lowers fasting blood glucose levels in the absence of eNOS, metformin (250 mg/kg) was injected intraperitoneally into streptozotocin-induced diabetic wild-type or *eNos*$^{-/-}$ mice. Characteristics of wild-type and *eNos*$^{-/-}$ mice used in the experiments showed no significant differences in body weight, fasting blood glucose levels or fed blood glucose levels before streptozotocin injection at 8 weeks of age among the four groups (Table 3).

Fasting blood glucose levels were lowered by about 3.9 mmol/l at 1 h after single administration of metformin in overnight-fasted wild-type diabetic mice, whereas those in overnight-fasted *eNos*$^{-/-}$ diabetic mice were not altered

Table 2 Effect of metformin on RNS production

Treatments	No addition	Addition of vitamins E and C
Control	1.03±0.01	0.94±0.01**
Metformin (2 mmol/l)	1.15±0.04*	0.95±0.01**
Rotenone (100 nmol/l)	1.03±0.02	0.99±0.01**
Hydrogen peroxide (300 μmol/l)	1.02±0.02	0.98±0.01**
$ONOO^-$ (10 μmol/l)	1.21±0.05*	1.00±0.01**

Data are expressed as the value at 60 min divided by the value at time zero (fold increase); values are means ± SE (n=8)

*p<0.05 vs control; **p<0.01 vs corresponding values without RNS scavengers

(Table 3). Administration of vehicle (saline) alone in overnight-fasted wild-type diabetic mice did not alter fasting blood glucose levels after single administration, as was also found in overnight-fasted *eNos*$^{-/-}$ diabetic mice (Table 3). Following the first injection, daily administration of metformin was continued for two more days. Administration of metformin for three consecutive days lowered fasting blood glucose levels by about 7.1 mmol/l in wild-type diabetic mice, whereas it had no lowering effect on fasting blood glucose in diabetic *eNos*$^{-/-}$ mice (Table 3). Administration of vehicle (saline) alone in overnight-fasted wild-type mice did not alter fasting blood glucose levels after administration for three consecutive days, as was also the case in *eNos*$^{-/-}$ mice (Table 3).

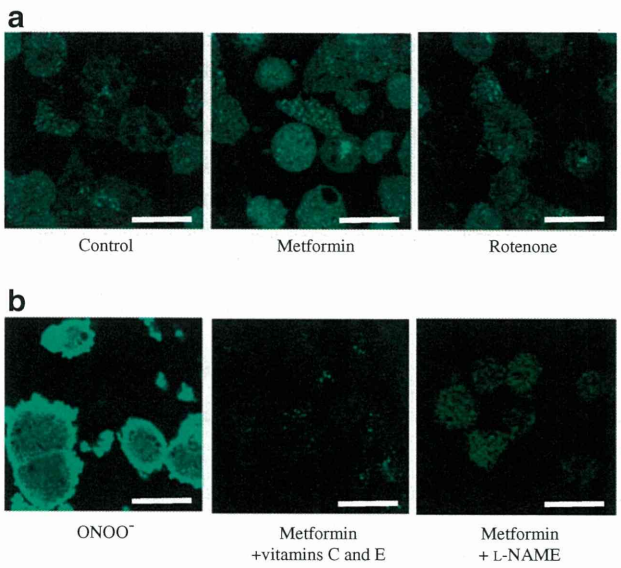

Fig. 2 Immunocytochemical staining with anti-nitrotyrosine antibody for detection of $ONOO^-$ generation. $ONOO^-$ (10 μmol/l) incubated for 5 min was used as a positive control. **a** Exposure to metformin (2 mmol/l) for 2 h increased staining, but exposure to rotenone (100 nmol/l) for the same time did not. **b** $ONOO^-$ generation induced by metformin was decreased by co-administration with RNS scavengers (5 mmol/l α-tocopherol [vitamin E] plus 2.3 mmol/l ascorbate [vitamin C]) and a NOS inhibitor (1 mmol/l L-NAME), respectively. Confocal microscopy, magnifications ×100; scale bars 50 μm

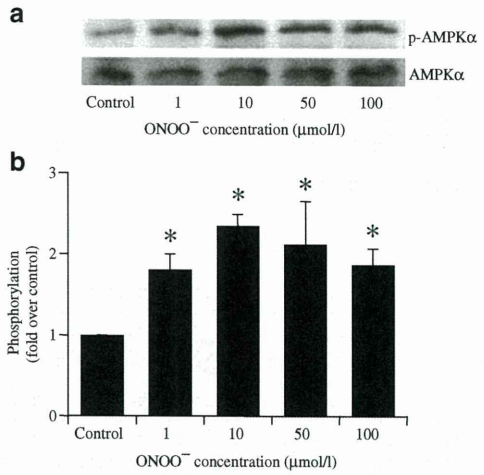

Fig. 3 Exogenous $ONOO^-$ stimulates AMPKα phosphorylation in freshly isolated hepatocytes. **a** Blot showing that direct exposure to $ONOO^-$ for 5 min at doses ranging from 1 to 100 μmol/l stimulated AMPKα phosphorylation. **b** Quantification with data expressed as fold stimulation over control. Values are means ± SE (n=4), *p<0.05 vs control

Lack of effects of metformin in vivo on AMPKα phosphorylation in liver tissues lacking eNOS In liver tissue samples collected after three consecutive days of administration, metformin stimulated phosphorylation of AMPKα in wild-type mice (metformin 2.17±0.30 [fold increase relative to vehicle], p<0.05 vs vehicle; Fig. 5a, b). However, stimulation of AMPKα phosphorylation by metformin was not observed in liver tissues of *eNos*$^{-/-}$ mice (metformin 0.97±0.12 [fold increase relative to vehicle], p=NS vs saline; Fig. 5a, c).

Discussion

In the present study, we show for the first time that activation of AMPK and the inhibitory effect on hepatic gluconeogenesis by metformin are mediated by generation of the RNS, $ONOO^-$. We also showed that eNOS plays an important role in metformin action in liver.

We investigated the metformin–RNS–AMPK pathway for its suppressing effects on hepatic gluconeogenesis. Because recent studies have shown that metformin activates AMPK through the RNS, $ONOO^-$, in BAEC [18], we evaluated RNS production in liver, the major target of metformin action. We found that metformin increased $ONOO^-$ generation and that $ONOO^-$ itself activates AMPK, which is induced in only 5 min. A previous study found that AMPK phosphorylation by metformin does not appear within 10 min but only after 30 min [31]. Consistent

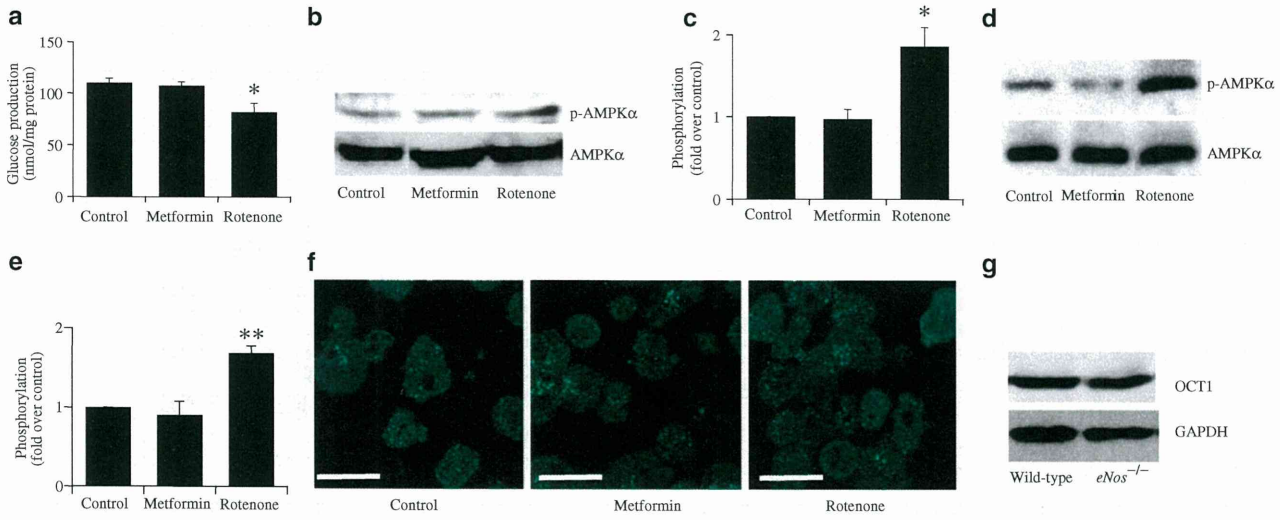

Fig. 4 Lack of effects of metformin on suppression of gluconeogenesis, AMPKα phosphorylation and $ONOO^-$ generation in hepatocytes lacking eNOS. **a** Metformin (2 mmol/l) did not suppress gluconeogenesis after 2 h exposure in hepatocytes lacking eNOS, but rotenone (100 nmol/l) suppressed gluconeogenesis to a similar degree to that observed in wild-type hepatocytes. Values are means ± SE (n=6), *p< 0.05 vs control. **b** Blot showing that AMPKα phosphorylation was not stimulated by metformin (2 mmol/l), but was stimulated by rotenone (100 nmol/l) after 2 h exposure in freshly isolated hepatocytes; (**c**) quantification with data expressed as fold stimulation over control. Values are means ± SE (n=4), *p<0.05 vs control. **d** Blot showing that AMPKα phosphorylation was not stimulated by metformin (2 mmol/l), but was stimulated by rotenone (100 nmol/l) after 2 h exposure in primary cultured hepatocytes, with (**e**) bar graph showing data expressed as fold stimulation over control. Values are means ± SE (n=5), **p<0.01 vs control. **f** Immunocytochemical staining (confocal microscopy) with anti-nitrotyrosine antibody in hepatocytes lacking eNOS. Exposure to metformin (2 mmol/l) and rotenone (100 nmol/l) for 2 h did not increase staining. Magnification ×100, scale bar 50 μm. **g** Levels of OCT1 protein in wild-type and *eNos*$^{-/-}$ mice hepatocytes. OCT1 levels in *eNos*$^{-/-}$ mice hepatocytes were similar to those in wild-type mice hepatocytes. Findings normalised to glyceraldehyde-3-phosphate dehydrogenase (GAPDH)

with that study, our data showed that AMPK phosphorylation by metformin did not appear within 15 min, but only after more than 30 min (data not shown). Thus, $ONOO^-$ generation appears to precede AMPK phosphorylation after exposure to metformin. $ONOO^-$ is generated by nitric oxide and superoxide anions; intra-hepatocellular nitric oxide is produced by NOS. In the present study, the NOS inhibitor, L-NAME, suppressed $ONOO^-$ production by metformin. This suggests that nitric oxide production by hepatocellular NOS is required for $ONOO^-$ production by metformin. Since eNOS is the representative subtype of the NOS family for generation of $ONOO^-$ in liver [17], we sought to determine whether eNOS is required for $ONOO^-$ production by metformin. Using eNOS-deficient mice, we were able to demonstrate that eNOS is essential for metformin action in liver. Thus metformin increases $ONOO^-$ produc-

Table 3 Effect of metformin on blood glucose levels in wild-type and *eNos*$^{-/-}$ diabetic mice

Treatments per mouse type	Pre streptozotocin			Post streptozotocin		
	Body weight (g)	FBG (mmol/l)	Fed BG (mmol/l)	FBG (mmol/l)	BG (mmol/l) at 1 h PM	FBG (mmol/l) after 3 days met
Wild-type mice						
Saline	20.3±0.4	3.7±0.2	8.2±0.5	16.0±2.7	17.2±3.1	16.6±3.3
Metformin	20.4±0.3	3.7±0.2	8.0±0.3	16.6±2.8	12.7±3.0**	9.5±1.9**
eNos$^{-/-}$ mice						
Saline	20.5±0.3	3.6±0.2	7.9±0.4	15.0±1.9	17.3±2.4	16.9±2.7
Metformin	20.7±0.3	3.5±0.2	8.1±0.5	15.8±1.6	19.0±1.9	16.5±2.1

Values are means ± SE (n=8)

**p<0.01 vs the value of pre-injection intraperitoneally with metformin in saline or saline only, paired t test

BG, blood glucose; FBG, fasting blood glucose; met, metformin; PM, post-metformin

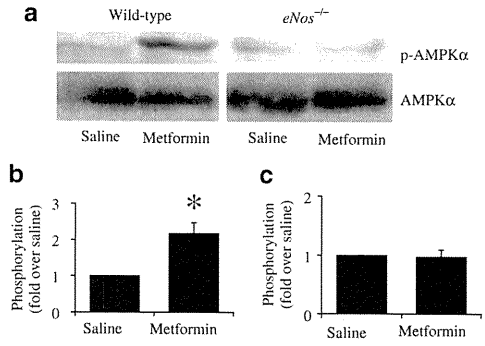

Fig. 5 Lack of effects of metformin in vivo on AMPKα phosphorylation in liver tissues deficient in eNOS. **a** Blot showing that metformin stimulated phosphorylation of AMPKα in liver tissues of wild-type diabetic mice after administration for three consecutive days. **b** Quantification of blot for wild-type and (**c**) *eNos*$^{-/-}$ mice. Metformin did not stimulate (**a, c**) phosphorylation of AMPKα in liver tissues of *eNos*$^{-/-}$ diabetic mice after metformin administration for three consecutive days. Data (**b, c**) are expressed as fold stimulation over saline. Values are means ± SE (n=5), *p<0.05 vs vehicle

tion, which is followed by AMPK activation and suppression of gluconeogenesis.

Although metformin has been reported not to affect the ATP content of hepatocytes [32], several studies have found that metformin decreased ATP content and/or increased the AMP/ATP ratio in hepatocytes [23, 33], possibly a result of metformin's suppressive effect on complex I activity in the respiratory chain [34] and one that plays an important role in AMPK activation by metformin. While metformin was found not to affect ATP content and the AMP/ATP ratio in the present study, the AMP/ATP ratio might nevertheless play an important role in AMPK activation by metformin because AMPK is sensitive to changes in the AMP/ATP ratio at levels too slight to be detected by measurement of the total adenine nucleotide content of whole cells [35]. Interestingly, metformin activates AMPK with a smaller increase in the AMP/ATP ratio than that effected by mitochondrial uncoupler and rosiglitazone [16] and without affecting the ADP/ATP ratio [10]. These results suggest that, apart from increases in the AMP/ATP ratio, other important mechanisms may be involved in AMP activation by metformin.

Rotenone inhibits complex I of the mitochondrial respiratory chain and decreases oxidative phosphorylation, leading to ATP depletion and an increase in the AMP/ATP ratio, which results in stimulation of AMPK phosphorylation. In the present study we observed that while 2 mmol/l metformin and 100 nmol/l rotenone had similar effects on gluconeogenesis and AMPK phosphorylation, the AMP/ATP ratio increased prominently only upon exposure to rotenone but not upon exposure to metformin. These results indicate that complex I inhibition alone is unlikely to explain the action of metformin. Interestingly, metformin significantly increased RNS in contrast to the lack of effect of rotenone on RNS. Furthermore, a decrease in metformin-induced RNS production by eNOS disruption abolished activation of AMPK by metformin. These results demonstrate that RNS is a regulator distinct from the AMP/ATP ratio in AMPK activation by metformin.

Some groups have reported that eNOS acts upstream of AMPK activation in BAEC [18], while other groups have reported that eNOS acts downstream of AMPK activation in capillary endothelial cells and in cardiomyocytes [21]. In the present study, we show that, in wild-type hepatocytes, direct exposure to $ONOO^-$ activates AMPK and that rotenone activates AMPK without increase in $ONOO^-$ production, supporting the former notion [18] in hepatocytes.

It is well known that high levels of RNS have deleterious effects on cell function and viability [17]. On the other hand, the low levels of RNS seen in physiological conditions are required for maintaining normal cell functions such as signal transduction [36]. For example, it has been reported that RNS production induced by skeletal muscle contraction is correlated with glucose uptake [20]. Thus, RNS has protective and damaging effects on cells. Indeed, the RNS produced by metformin at a dose used in the present study (2 mmol/l) should have beneficial effects on hepatic glucose metabolism through AMPK activation.

We demonstrate in the present study that AMPK activation by metformin in hepatocytes is dependent on RNS. We also demonstrate that eNOS plays an important role in suppressing hepatic gluconeogenesis in vitro as well as in lowering fasting blood glucose levels in vivo. It is generally accepted that fasting blood glucose levels are determined by hepatic gluconeogenesis, which suggests that eNOS is required for metformin's action on fasting blood glucose levels.

In the present study, we have elucidated a novel mechanism for metformin action. However, some limitations of this study must be considered. In our in vivo metformin experiments, the mice were injected intraperitoneally with 250 mg/kg metformin in 0.9% sterile saline, which is a similar dosage to that used previously [8, 18]. This protocol using a high dose of metformin for rodents may cause a very distinct acute response. Therefore, we cannot exclude the possibility that the acute hepatocellular response to AMPK activation by metformin in the present study differs from the clinical effects of metformin when used to treat patients with type 2 diabetes. To elucidate the detailed mechanisms of AMPK activation by metformin in liver, which may provide novel therapeutic targets for type 2 diabetes, further investigations are required.

Acknowledgements This study was supported by Scientific Research Grants, a Grant for Leading Project for Biosimulation from the Ministry of Education, Culture, Sports, Science and Technology of Japan, and by a grant from CREST of Japan Science and Technology Cooperation. Support was also provided in the form of a grant from the Ministry of Health, Labor and Welfare, Japan, and also by Kyoto University Global COE Program 'Center for Frontier Medicine'.

Duality of interest The authors declare that there is no duality of interest associated with this manuscript.

References

1. Nathan DM, Buse JB, Davidson MB et al (2008) Management of hyperglycaemia in type 2 diabetes mellitus: a consensus algorithm for the initiation and adjustment of therapy. Update regarding the thiazolidinediones. Diabetologia 51:8–11
2. Nathan DM, Buse JB, Davidson MB et al (2006) Management of hyperglycaemia in type 2 diabetes: a consensus algorithm for the initiation and adjustment of therapy. A consensus statement from the American Diabetes Association and the European Association for the Study of Diabetes. Diabetologia 49:1711–1721
3. Inzucchi SE, Maggs DG, Spollett GR et al (1998) Efficacy and metabolic effects of metformin and troglitazone in type II diabetes mellitus. N Engl J Med 338:867–873
4. Scarpello JH, Howlett HC (2008) Metformin therapy and clinical uses. Diab Vasc Dis Res 5:157–167
5. Bailey CJ (1992) Biguanides and NIDDM. Diabetes Care 15:755–772
6. UK Prospective Diabetes Study (UKPDS) Group (1998) Effect of intensive blood-glucose control with metformin on complications in overweight patients with type 2 diabetes (UKPDS 34). Lancet 352:854–865
7. Brunmair B, Staniek K, Gras F et al (2004) Thiazolidinediones, like metformin, inhibit respiratory complex I. Diabetes 53:1052–1059
8. Shaw RJ, Lamia KA, Vasquez D et al (2005) The kinase LKB1 mediates glucose homeostasis in liver and therapeutic effects of metformin. Science 310:1642–1646
9. Zhou G, Myers R, Li Y, Chen Y et al (2001) Role of AMP-activated protein kinase in mechanism of metformin action. J Clin Invest 108:1167–1174
10. Hawley SA, Gadalla AE, Olsen GS, Hardie DG (2002) The antidiabetic drug metformin activates the AMP-activated protein kinase cascade via an adenine nucleotide-independent mechanism. Diabetes 51:2420–2425
11. Tian R, Musi N, D'Agostino J, Hirshman MF, Goodyear LJ (2001) Increased adenosine monophosphate-activated protein kinase activity in rat hearts with pressure-overload hypertrophy. Circulation 104:1664–1669
12. Hardie DG (2004) The AMP-activated protein kinase pathway—new players upstream and downstream. J Cell Sci 117:5479–5487
13. Hardie DG, Hawley SA, Scott JW (2006) AMP-activated protein kinase—development of the energy sensor concept. J Physiol 574: 7–15
14. El-Mir MY, Nogueira V, Fontaine E, Ave'ret N, Rigoulet M, Leverve X (2000) Dimethylbiguanide inhibits cell respiration via an indirect effect targeted on the respiratory chain complex I. J Biol Chem 275:223–228
15. Owen MR, Doran E, Halestrap AP (2000) Evidence that metformin exerts its anti-diabetic effects through inhibition of complex 1 of the mitochondrial respiratory chain. Biochem J 348:607–614
16. Fryer LG, Parbu-Patel A, Carling D (2002) The anti-diabetic drugs rosiglitazone and metformin stimulate AMP-activated protein kinase through distinct signaling pathways. J Biol Chem 277:25226–25232
17. Pacher P, Beckman JS, Liaudet L (2007) Nitric oxide and $ONOO^-$ in health and disease. Physiol Rev 87:315–424
18. Zou MH, Kirkpatrick SS, Davis BJ et al (2004) Activation of the AMP-activated protein kinase by the anti-diabetic drug metformin in vivo. Role of mitochondrial reactive nitrogen species. J Biol Chem 279:43940–43951
19. Davis BJ, Xie Z, Viollet B, Zou MH (2006) Activation of the AMP-activated kinase by antidiabetes drug metformin stimulates nitric oxide synthesis in vivo by promoting the association of heat shock protein 90 and endothelial nitric oxide synthase. Diabetes 55:496–505
20. Ross RM, Wadley GD, Clark MG, Rattigan S, McConell GK (2007) Local nitric oxide synthase inhibition reduces skeletal muscle glucose uptake but not capillary blood flow during in situ muscle contraction in rats. Diabetes 56:2885–2892
21. Chen ZP, Mitchelhill KI, Michell BJ et al (1999) AMP-activated protein kinase phosphorylation of endothelial NO synthase. FEBS Lett 443:285–289
22. Fujiwara H, Hosokawa M, Zhou X et al (2008) Curcumin inhibits glucose production in isolated mice hepatocytes. Diabetes Res Clin Pract 80:185–191
23. Argaud D, Roth H, Wiernsperger N, Leverve XM (1993) Metformin decreases gluconeogenesis by enhancing the pyruvate kinase flux in isolated rat hepatocytes. Eur J Biochem 213:1341–1348
24. Kooy NW, Royall JA, Ischiropoulos H (1997) Oxidation of 2′,7′-dichlorofluorescin by $ONOO^-$. Free Radic Res 27:245–254
25. Crow JP (1997) Dichlorodihydrofluorescein and dihydrorhodamine 123 are sensitive indicators of $ONOO^-$ in vitro: implications for intracellular measurement of reactive nitrogen and oxygen species. Nitric Oxide 2:145–157
26. Possel H, Noack H, Augustin W, Keilhoff G, Wolf G (1997) 2,7-Dihydrodichlorofluorescein diacetate as a fluorescent marker for $ONOO^-$ formation. FEBS Lett 416:175–178
27. Kominato R, Fujimoto S, Mukai E et al (2008) Src activation generates reactive oxygen species and impairs metabolism-secretion coupling in diabetic Goto–Kakizaki and ouabain-treated rat pancreatic islets. Diabetologia 51:1226–1235
28. Nabe K, Fujimoto S, Shimodahira M et al (2006) Diphenylhydantoin suppresses glucose-induced insulin release by decreasing cytoplasmic H^+ concentration in pancreatic islets. Endocrinology 147:2717–2727
29. Fujimoto S, Mukai E, Hamamoto Y et al (2002) Prior exposure to high glucose augments depolarization-induced insulin release by mitigating the decline of ATP level in rat islets. Endocrinology 143:213–221
30. Shu Y, Sheardown SA, Brown C et al (2007) Effect of genetic variation in the organic cation transporter 1 (OCT1) on metformin action. J Clin Invest 117:1422–1431
31. Xie Z, Dong Y, Scholz R, Neumann D, Zou MH (2008) Phosphorylation of LKB1 at serine 428 by protein kinase C-ζ is required for metformin-enhanced activation of the AMP-activated protein kinase in endothelial cells. Circulation 117: 952–962
32. Wollen N, Bailey CJ (1988) Inhibition of hepatic gluconeogenesis by metformin. Synergism with insulin. Biochem Pharmacol 37:4353–4358
33. Guigas B, Bertrand L, Taleux N et al (2006) 5-Aminoimidazole-4-carboxamide-1-beta-D-ribofuranoside and metformin inhibit

hepatic glucose phosphorylation by an AMP-activated protein kinase-independent effect on glucokinase translocation. Diabetes 55:865–874

34. Hinke SA, Martens GA, Cai Y et al (2007) Methyl succinate antagonises biguanide-induced AMPK-activation and death of pancreatic beta-cells through restoration of mitochondrial electron transfer. Br J Pharmacol 150:1031–1043
35. Zhang L, He H, Balschi JA (2007) Metformin and phenformin activate AMP-activated protein kinase in the heart by increasing cytosolic AMP concentration. Am J Physiol Heart Circ Physiol 293:H457–H466
36. Bashan N, Kovsan J, Kachko I, Ovadia H, Rudich A (2009) Positive and negative regulation of insulin signaling by reactive oxygen and nitrogen species. Physiol Rev 89:27–71

Exendin-4 Protects Pancreatic Beta Cells from the Cytotoxic Effect of Rapamycin by Inhibiting JNK and p38 Phosphorylation

Authors

Y. Kawasaki[1], S. Harashima[1], M. Sasaki[1], E. Mukai[1,2], Y. Nakamura[1], N. Harada[1], K. Toyoda[1], A. Hamasaki[1], S. Yamane[1], C. Yamada[1], Y. Yamada[1,3], Y. Seino[1,4], N. Inagaki[1,5]

Affiliations

Affiliation addresses are listed at the end of the article

Key words
- exendin-4
- rapamycin
- JNK
- p38
- beta cells

Abstract

It has been reported that the immunosuppressant rapamycin decreases the viability of pancreatic beta cells. In contrast, exendin-4, an analogue of glucagon-like peptide-1, has been found to inhibit beta cell death and to increase beta cell mass. We investigated the effects of exendin-4 on the cytotoxic effect of rapamycin in beta cells. Incubation with 10 nM rapamycin induced cell death in 12 h in murine beta cell line MIN6 cells and Wistar rat islets, but not when coincubated with 10 nM exendin-4. Rapamycin was found to increase phosphorylation of c-Jun amino-terminal kinase (JNK) and p38 in 30 minutes in MIN6 cells and Wistar rat islets while exendin-4 decreased their phosphorylation. Akt and extracellular signal-regulated kinase (ERK) were not involved in the cytoprotective effect of exendin-4. These results indicate that exendin-4 may exert its protective effect against rapamycin-induced cell death in pancreatic beta cells by inhibiting JNK and p38 signaling.

Introduction

Exendin-4 is presently being used in patients with type 2 diabetes [1]. The glucagon-like peptide-1 (GLP-1) analogue improves blood glucose levels by increasing insulin secretion. Exendin-4 is also suggested to promote beta cell proliferation and neogenesis and to inhibit beta cell apoptosis, thereby increasing beta cell mass, at least in rodents [2]. Apoptosis induced by inflammatory cytokines [3] or endoplasmic reticulum (ER) stress [4] was shown to be prevented by exendin-4 in primary rat beta cells and INS-1, a murine beta cell line. Treatment with exendin-4 markedly attenuates beta cell apoptosis in db/db mice [5] and in male C57BL/6 mice exposed to streptozotocin [6]. The molecular mechanism of the cytoprotective effect of exendin-4 is mediated by increased levels of cyclic AMP (cAMP) that lead to activation of protein kinase A (PKA), enhanced insulin receptor substrate-2 (IRS-2) activity, and activation of Akt and extracellular signal-regulated kinase (ERK) [7]. Recently it was reported that exendin-4 inhibits cytokine-induced apoptosis, which involves electron transport chain proteins of mitochondria with a reduction of oxidative stress in INS-1 cells [8].

Rapamycin, an immunosuppressant used to prevent rejection in organ transplantation, is reported to impair glucose-stimulated insulin secretion in rat islets and to decrease viability of rat and human islets [9]. A recent study suggested that rapamycin reduces beta cell mass by 50% under diabetic conditions in *Psammomys obesus*, an animal model of nutrition-dependent type 2 diabetes, by increasing c-Jun amino-terminal kinase (JNK) phosphorylation [10].

We investigated whether exendin-4 might ameliorate the cytotoxic effects of rapamycin. In the present study, we found that rapamycin induces cell death in beta cells through an increase in phosphorylation of JNK and p38, and that exendin-4 prevents such rapamycin-induced cell death by inhibiting these molecules.

Materials and Methods

Materials

Tissue culture media, DMEM and RPMI1640, rapamycin, exendin-4, exendin (9–39) (exendin-9), H89, LY294002, PD98059, SP600125, SB203580, RNaseA, propidium iodide (PI), and anti-α-tubulin antibody (Ab) were obtained from Sigma Aldrich (St Louis, MO, USA). Fetal bovine

received 19.09.2009
accepted 08.02.2010

Bibliography
DOI http://dx.doi.org/10.1055/s-0030-1249035
Published online: 2010
Horm Metab Res

ISSN 0018-5043

Correspondence
N. Inagaki, MD, PhD
Department of Diabetes and Clinical Nutrition
Graduate School of Medicine
Kyoto University
54 Shogoin Kawahara-cho
Sakyo-ku
606-8507 Kyoto
Japan
Tel.: +81/75/751 3560
Fax: +81/75/771 6601
inagaki@metab.kuhp.kyoto-u.ac.jp

serum (FBS) was from Invitrogen (Carlsbad, CA, USA). Anti-phospho-Akt (Ser473) Ab, anti-Akt Ab, anti-phospho-JNK (Thr183/Tyr185) Ab, anti-JNK Ab, anti-phospho-p38 (Thr180/Tyr182) Ab, anti-p38 Ab, anti-caspase-3 Ab, and anti-cleaved caspase-3 Ab were obtained from Cell Signaling (Danvers, MA, USA). Anti-phospho-ERK Ab and anti-ERK Ab were from Santa Cruz Biotechnology (Santa Cruz, CA, USA).

Methods

Cell culture and stimulation of MIN6 cells

MIN6 cells were maintained in 25 mM glucose DMEM media supplemented with 13% FBS, 100 U/ml penicillin, 100 µg/ml streptomycin, and 5 µl β-mercaptoethanol at 37 °C in humidified air containing 5% CO_2. For the experiment, the cells (1.2×10^6) were plated into 35 mm dishes, incubated in DMEM media with or without protein kinase inhibitors for 30 min, and rapamycin and/or exendin-4, and/or forskolin, and/or exendin-9 were then added into the media. After the indicated time periods, the cells were collected and analyzed for cell death and protein phosphorylation.

Islet isolation and stimulation

Pancreatic islets were isolated from Wistar rats by collagenase digestion as described previously [11], and preincubated in RPMI 1640 medium containing 10% FBS, 100 U/ml penicillin, 100 µg/ml streptomycin, and 5.5 mM glucose at 37 °C in humidified air containing 5% CO_2 for 60 min. After preincubation, the islets were cultured in the media with 10 nM rapamycin and/or 10 nM exendin-4 for the indicated time periods and then analyzed for cell death, protein phosphorylation, and insulin secretion and content.

Insulin secretion and content

Insulin secretion from islets was monitored using batch incubation as previously described [11]. After islets were cultured with 10 nM rapamycin and/or 10 nM exendin-4 for 12 h, the islets were collected, washed, and preincubated at 37 °C for 30 min in Krebs-Ringer bicarbonate buffer (KRBB) medium supplemented with 2.8 mM glucose, and groups of 5 islets were then batch-incubated for 30 min in 0.7 ml KRBB medium containing 2.8 mM and 16.7 mM glucose. At the end of the incubation period, the islets were pelleted by centrifugation, and aliquots of the buffer were sampled to determine the amount of immunoreactive

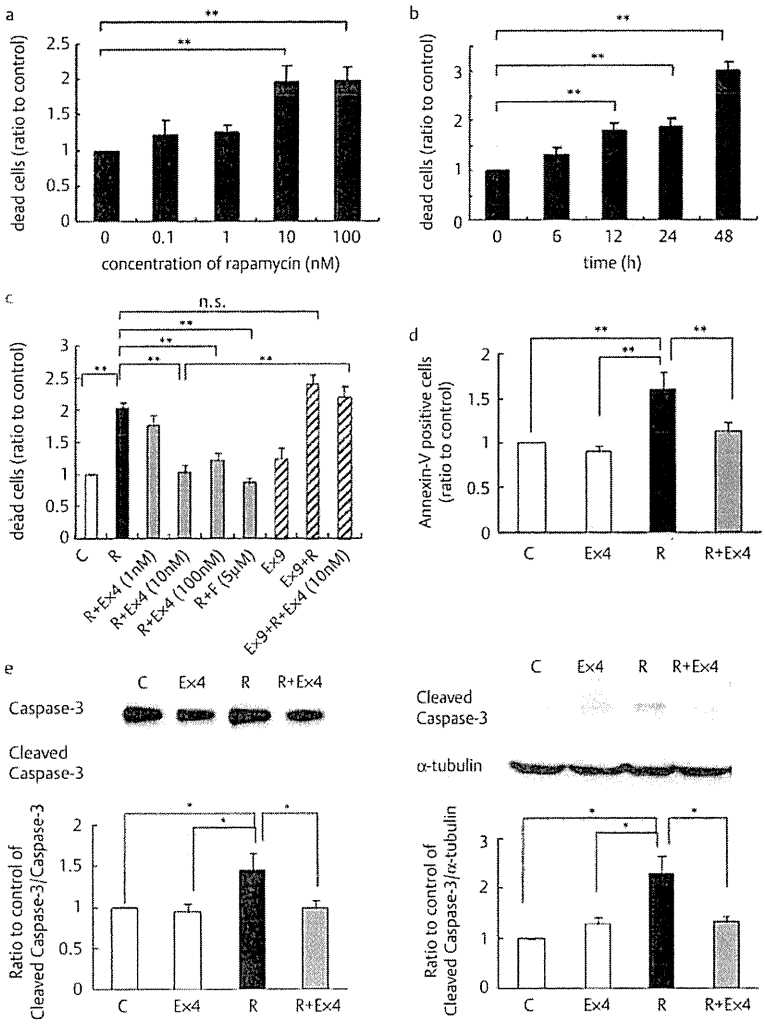

Fig. 1 Exendin-4 inhibits rapamycin-induced cell death in MIN6 cells. **a**: Dose-dependency and **b**: time-dependency of rapamycin-induced cell death in MIN6 cells. MIN6 cells were treated with 0.1, 1, 10, or 100 nM rapamycin for 12 h (**a**) or with 10 nM rapamycin for 6, 12, 24, or 48 h (**b**), and dead cells with sub-G1 DNA content were counted by flowcytometer. Data are means ± SE of five independent experiments. ** $p < 0.01$. **c**: Quantification of dead cells 12 h after treatment with DMSO (control), 10 nM rapamycin, 10 nM rapamycin and 1, 10, or 100 nM exendin-4, 10 nM rapamycin and 5 µM forskolin, 100 nM exendin-9, and 100 nM exendin-9 and 10 nM rapamycin with or without 10 nM exendin-4. Data are means ± SE of four independent experiments. ** $p < 0.01$. **d**: The percentage of annexin-V-FITC positive cells. MIN6 cells were cultured with 10 nM rapamycin and/or 10 nM exendin-4, and annexin-V-FITC positive cells were counted by flowcytometer. Data are means ± SE of three independent experiments. ** $p < 0.01$. **e**: Western blot analysis of caspase-3 and cleaved caspase-3 in MIN6 cells treated with 10 nM rapamycin and/or 10 nM exendin-4 for 12 h. Images are representative of three independent experiments. Graphs show relative ratio of cleaved caspase-3 versus caspase-3 or α-tubulin, respectively. * $p < 0.05$. C: control (DMSO); R: rapamycin; Ex4: exendin-4; F: forskolin; Ex9: exendin-9.

insulin by RIA. After an aliquot of incubation medium for insulin release assay in 2.8 mM glucose was taken, the remaining islets were lysed and insulin contents were determined.

Quantification of cell death

MIN6 cells incubated under the conditions indicated were collected from both attached and floating cell populations and fixed with 70% ethanol for 4 h. The cells were then washed with PBS, incubated in phosphate-citrate buffer for 30 min, resuspended in 10 µg/ml RNaseA containing PBS, and stained with 10 µg/ml PI. Dead cells containing sub-G1 DNA content were identified and analyzed by a FACS Calibur instrument (BD Biosciences, San Jose, CA, USA). Annexin-V positive cells were analyzed by FACS Calibur using annexin-V-FITC Apoptosis Detection Kit (BD Pharmingen, San Diego, CA, USA). Primary islets were cultured in the indicated conditions for 12 h. DNA fragmentation was measured by quantification of cytosolic oligonucleosome-bound DNA using Cell Death Detection ELISA (Roche, Mannheim, Germany) as previously described [12]. To detect caspase-3 activity, MIN6 cells and primary islets were cultured with 10 nM rapamycin and/or 10 nM exendin-4 for 12 h, and 50 µg of the proteins were subjected to western blot analysis.

Western blot analysis

Cells were collected and washed twice with PBS, and then sonicated in lysis buffer. Equivalent amounts of protein were resolved by SDS/PAGE on 4–12% acrylamide gels (Invitrogen) and transferred to PVDF membranes (Invitrogen), followed by immunoblotting with antibodies to detect respective proteins.

Fluorescence labeling with Newport Green

Islet beta cells from Wistar rat were cultured with 10 nM rapamycin and/or 10 nM exendin-4 for 12 h and stained with Newport Green (Invitrogen) for 30 min. The labeled beta cells were visualized by fluorescence microscopy (Keyence, New Jersey, USA).

Statistics

Data are expressed as mean ± SE. Statistical comparisons were made between groups using one-way analysis of variance. Significant differences were evaluated using Tukey-Kramer post hoc analysis.

Results

Exendin-4 inhibits rapamycin-induced cell death in MIN6 cells

We first examined the dose-dependency and time-dependency of rapamycin-induced cell death in MIN6 cells. The number of dead cells was significantly increased in 10 and 100 nM rapamycin-treated MIN6 cells compared to that in DMSO-treated cells (control) in 12 h (◎ **Fig. 1a**). The number of dead cells induced by 10 nM rapamycin, a therapeutic concentration in blood [13], was significantly increased from 12 h and maximized at 48 h (◎ **Fig. 1b**), indicating cytotoxicity in MIN6 cells in 12 h.

MIN6 cells were then treated with 1, 10, or 100 nM exendin-4 in the presence of 10 nM rapamycin for 12 h. The number of rapamycin-induced dead cells was significantly reduced by 97.0 ± 14.9% and 78.1 ± 14.5% by coincubation with 10 and 100 nM exendin-4, respectively (◎ **Fig. 1c**). In addition, 5 µM forskolin, an adenylyl cyclase activator, completely blocked rapamycin-induced cell death (◎ **Fig. 1c**). In addition, exendin-9, an

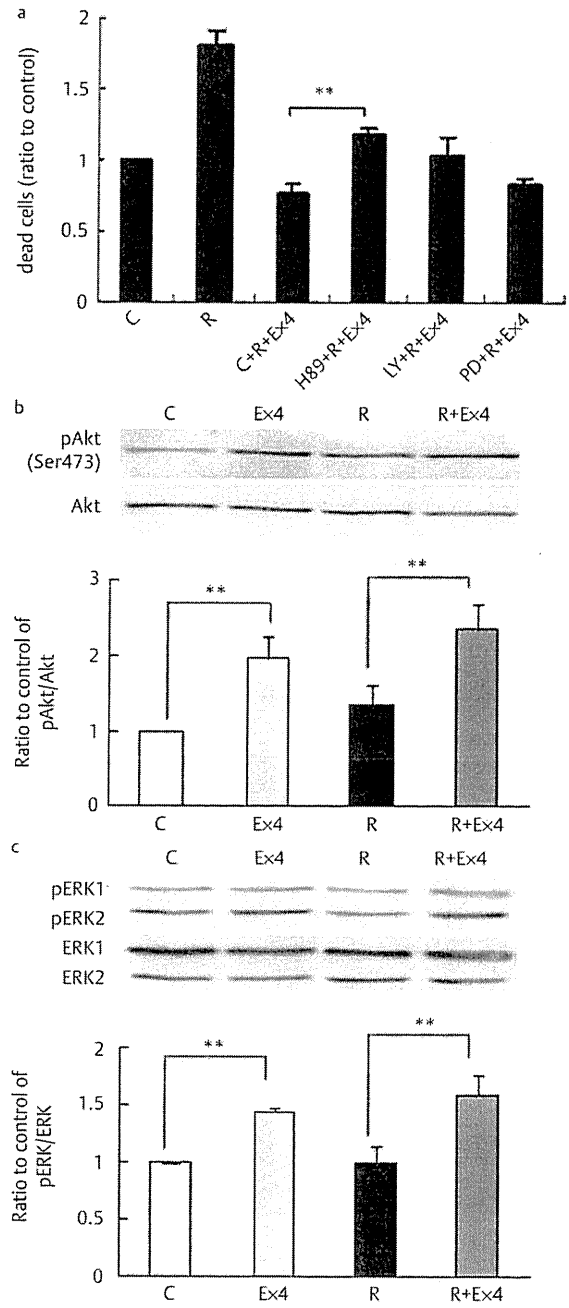

Fig. 2 Cytoprotective effect of exendin-4 is partially mediated by PKA, but not by PI3K/Akt and ERK. a: The percentage of dead cells with sub-G1 DNA content. DMSO (control), 15 µM H89, 10 µM LY294002, or 50 µM PD98059 was added into the media 30 min before treatment with 10 nM rapamycin and 10 nM exendin-4 for 12 h in MIN6 cells, and dead cells were counted by flowcytometer. Data are means ± SE of four independent experiments. ** $p < 0.01$. b, c: Western blot analysis of Akt and ERK in MIN6 cells treated with 10 nM rapamycin and/or 10 nM exendin-4 for 30 min. Images are representative of three independent experiments. Graphs show relative ratio of phosphorylated Akt or ERK vs. total Akt or ERK, respectively, by treatment with rapamycin and/or exendin-4 compared to control (DMSO). Data are means ± SE of three independent experiments. ** $p < 0.01$. C: control (DMSO); R: rapamycin; Ex4: exendin-4; LY: LY294002; PD: PD98059.

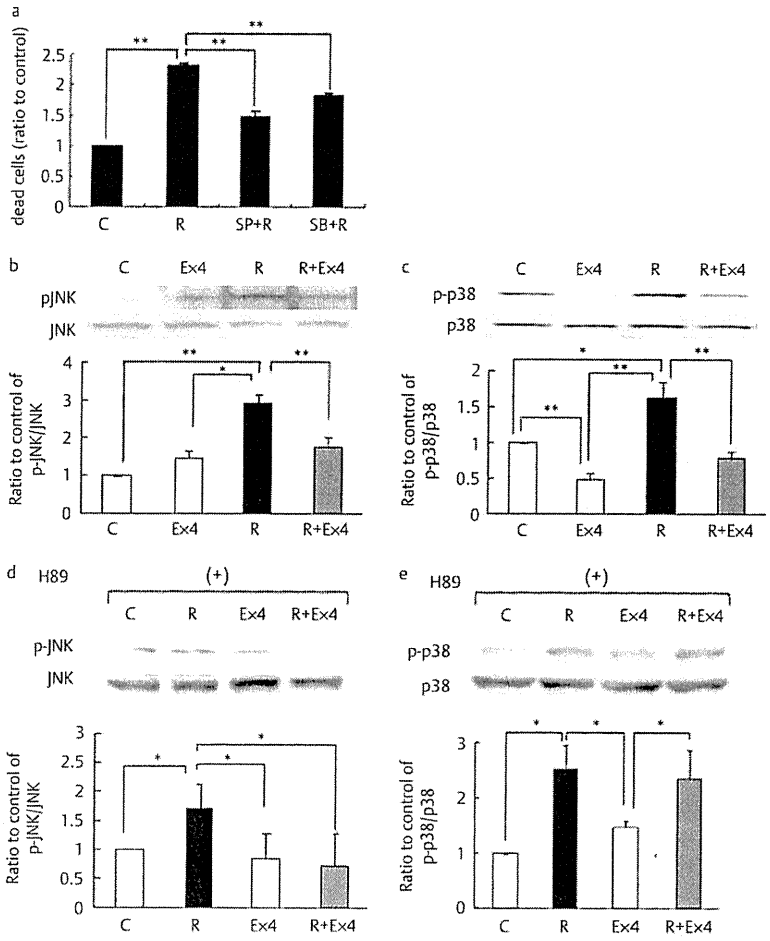

Fig. 3 Exendin-4 inhibits rapamycin-induced cell death by decreasing JNK and p38 phosphorylation in MIN6 cells. **a:** The percentage of dead cells with sub-G1 DNA content. DMSO (control), 10 μM SP600125 or 10 μM SB203580 was added into MIN6 cells 30 min before treatment with 10 nM rapamycin for 12 h, and dead cells were counted by flowcytometer. Data are means ± SE of four independent experiments. ** $p<0.01$.
b, c: Western blot analysis of JNK and p38 in MIN6 cells treated with 10 nM rapamycin and/or 10 nM exendin-4 for 30 min. **d, e:** Western blot analysis of JNK and p38 in MIN6 cells to which 15 μM H89 was added 30 min before incubation with 10 nM rapamycin and/or 10 nM exendin-4 for 30 min. Images are representative of three independent experiments. Graphs show relative ratio of phosphorylated JNK or p38 v.s. total JNK or p38, respectively, by treatment with rapamycin and/or exendin-4 compared to control (DMSO). Data are means ± SE of three independent experiments. * $p<0.05$ ** $p<0.01$. C: control (DMSO); R: rapamycin; Ex4: exendin-4; SP: SP600125; SB: SB203580.

antagonist of the GLP-1 receptor, inhibited the cytoprotective effect of exendin-4 on rapamycin-induced cell death (◎ **Fig. 1c**). Annexin-V-positive apoptotic cells were also significantly increased in rapamycin-treated MIN6 cells compared to those in control cells, which increase was prevented by treatment with exendin-4 (◎ **Fig. 1d**). Furthermore, rapamycin increased caspase-3 activity, while exendin-4 decreased it in rapamycin-treated MIN6 cells (◎ **Fig. 1e**). These results indicate that exendin-4 inhibits rapamycin-induced cell death through the GLP-1 receptor by an increase in the intracellular cAMP concentration in MIN6 cells.

Cytoprotective effect of exendin-4 is mediated in part by PKA, but not by PI3K and ERK

We then examined the involvement of PKA, phosphatidylinositol 3-kinase (PI3K)/Akt, and ERK, downstream molecules of the GLP-1 receptor signaling pathways. DMSO (control), 15 μM H89, a PKA inhibitor, 10 μM LY294002, a PI3K inhibitor, or 50 μM PD98059, an ERK inhibitor, was added into the media 30 min before treatment with 10 nM exendin-4 and 10 nM rapamycin for 12 h in MIN6 cells, and dead cells were counted by flowcytometer. H89, a PKA inhibitor, partially but significantly blocked the cytoprotective effect of exendin-4 (◎ **Fig. 2a**). On the other hand, neither LY294002 nor PD98059 altered the cytoprotective effect of exendin-4 against rapamycin-induced cell death (◎ **Fig. 2a**), although phosphorylation of Akt and ERK was significantly increased by treatment with exendin-4 (◎ **Fig. 2b** and **c**). These results indicate that PKA is involved, at least in part, in the cytoprotective effect of exendin-4 against rapamycin-induced cell death.

JNK and p38 are involved in rapamycin-induced cell death in MIN6 cells

Previous studies found that rapamycin induces apoptosis in rh30, a human rhabdomyosarcoma cell line [14], and in islets isolated from *P. Obesus* [10], by activating JNK. In contrast, rapamycin inhibits palmitate-induced ER stress and apoptosis in INS-1E cells [15]. To clarify the involvement of JNK in rapamycin-induced cytotoxicity in MIN6 cells, 10 μM SP600125, a JNK inhibitor, was added into the media 30 min before treatment with 10 nM rapamycin for 12 h, when dead cells were counted by flowcytometer. SP600125 significantly inhibited rapamycin-induced cell death by 62.6 ± 9.1% (◎ **Fig. 3a**). We also examined the involvement of p38, the other stress-activated protein kinase [16]. Ten μM SB203580, a p38 inhibitor, added to MIN6 cells 30 min before treatment with 10 nM rapamycin for 12 h resulted in significant inhibition of rapamycin-induced cell death by 36.8 ± 6.4% (◎ **Fig. 3a**). These results indicate that rapamycin-induced cell death is mediated by JNK and p38 in MIN6 cells.

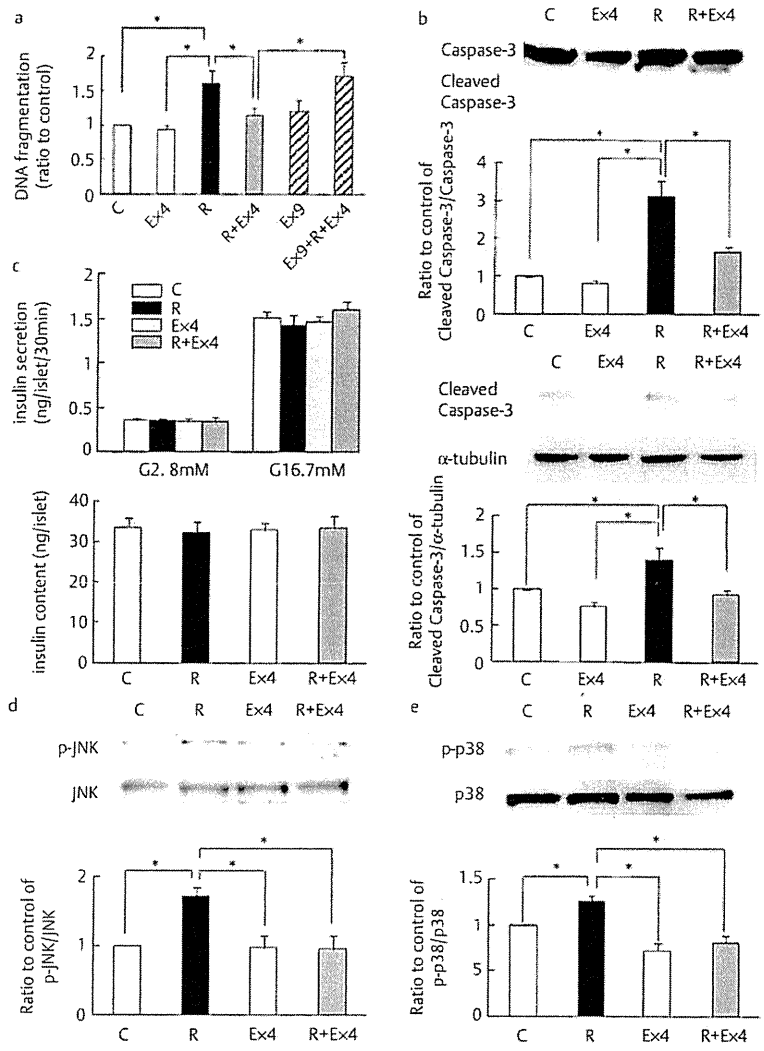

Fig. 4 Exendin-4 inhibits cell death and phosphorylation of JNK and p38 induced by rapamycin in Wistar rat primary islets. **a**: Primary islets were treated with 10 nM rapamycin and/or 10 nM exendin-4 and/or 100 nM exendin-9 for 12 h, and dead cells were detected by DNA fragmentation. Data are means ± SE of three independent experiments. * $p < 0.05$ **b**: Western blot analysis of caspase-3 and cleaved caspase-3 in primary islets treated with 10 nM rapamycin and/or 10 nM exendin-4 for 12 h. Images are representative of three independent experiments. Graphs show relative ratio of cleaved caspase-3 v.s. caspase-3 or α-tubulin, respectively. * $p < 0.05$. **c**: Glucose-stimulated insulin secretion and insulin content in Wistar rat islets treated with 10 nM rapamycin and/or 10 nM exendin-4 for 12 h. Data are means ± SE of three independent experiments. **d, e**: Primary islets were treated with 10 nM rapamycin and/or 10 nM exendin-4 for 30 min, and phosphorylation of JNK and p38 was detected by western blot. Images are representative of three independent experiments. Graphs show relative ratio of phosphorylated JNK or p38 vs. total JNK or p38, respectively, by treatment with rapamycin and/or exendin-4 compared to control (DMSO). Data are means ± SE of four independent experiments. * $p < 0.05$. C: control (DMSO); R: rapamycin; Ex4: exendin-4; Ex9: exendin-9; G: glucose.

Exendin-4 inhibits phosphorylation of JNK and p38 induced by rapamycin

To confirm the involvement of JNK and p38 in rapamycin-induced cell death, MIN6 cells were incubated with 10 nM rapamycin for 30 min, and phosphorylation of JNK and p38 was detected by western blot analysis. Phosphorylation of JNK and p38 was significantly increased 2.9 ± 0.2-fold and 1.6 ± 0.3-fold, respectively, compared to that in nontreated cells (⊙ **Fig. 3b** and **c**). In contrast, 10 nM exendin-4 decreased phosphorylation of both JNK and p38 in rapamycin-treated MIN6 cells (⊙ **Fig. 3b** and **c**). However, rapamycin and exendin-4 were found not to affect phosphorylation of mitogen-activated protein kinase kinase (MKK) 3/6, a kinase of p38, or MKK4, a kinase of JNK (data not shown), indicating that dephosphorylation of both JNK and p38 by exendin-4 is not mediated by these upstream kinases.

PKA is involved in dephosphorylation of p38 by exendin-4

Because PKA partially inhibited rapamycin-induced cell death, we examined the effect of H89 on JNK and p38 phosphorylation. Fifteen μM H89 was added into the media of MIN6 cells 30 min before treatment with 10 nM rapamycin and/or 10 nM exendin-4 for 30 min, when phosphorylation of JNK and p38 was detected by western blot analysis. H89 did not affect decreased phosphorylation of JNK by exendin-4 (⊙ **Fig. 3d**). By contrast, H89 significantly inhibited dephosphorylation of p38 by exendin-4 (⊙ **Fig. 3e**), indicating that PKA regulates p38 phosphorylation.

Exendin-4 inhibits rapamycin-induced cell death and phosphorylation of JNK and p38 in Wistar rat islets

We lastly investigated whether exendin-4 inhibits cell death induced by rapamycin in primary islets by affecting phosphorylation of JNK or p38. Wistar rat islets were treated with 10 nM rapamycin and/or 10 nM exendin-4 for 12 h, and the number of dead cells was determined by DNA fragmentation. Rapamycin significantly increased DNA fragmentation by 1.6 ± 0.2-fold compared to that of control (DMSO) (⊙ **Fig. 4a**), while exendin-4 significantly inhibited rapamycin-induced DNA fragmentation (⊙ **Fig. 4a**). Exendin-9 again completely blocked the cytoprotective effect of exendin-4 (⊙ **Fig. 4a**), indicating that such cytoprotective effect of exendin-4 is mediated by the GLP-1 receptor in primary islets. Caspase-3 activity also was significantly increased in rapamycin-treated islets, which was prevented by treatment with exendin-4 (⊙ **Fig. 4b**). To determine whether the surviving

cells treated with exendin-4 were actually beta cells, islet beta cells were stained with Newport Green, a fluorescent indicator of zinc that allowed visualization of islet beta cells [17] after treatment with 10 nM rapamycin and/or 10 nM exendin-4 for 12 h. Fluorescence microscopy revealed Newport Green positive cells treated with rapamycin and exendin-4 that are almost the same as those treated with DMSO (control) or exendin-4 alone (data not shown). In addition, insulin content and glucose-stimulated insulin secretion (GSIS) were compared among rapamycin- and/or exendin-4-treated Wistar rat islets to determine whether or not these islets are still functional. After islets were incubated with 10 nM rapamycin and/or 10 nM exendin-4 for 12 h, the rapamycin and exendin-4 were washed out and the islets were then stimulated with 2.8 mM or 16.7 mM glucose for 30 min. The amounts of GSIS and insulin content were almost the same in rapamycin- and exendin-4-treated islets, indicating that islets treated with rapamycin and exendin-4 for 12 h are still functional (◎ **Fig. 4c**).

Finally, regulation of JNK and p38 by rapamycin or exendin-4 in primary islets was examined. Incubation with 10 nM rapamycin for 30 min significantly increased phosphorylation of JNK and p38 by 1.7±0.2-fold and 1.3±0.1-fold, respectively, which was reversed to control level by coincubation with exendin-4 (◎ **Fig. 4d** and **e**). These results indicate that exendin-4 protects primary islets from rapamycin-induced cytotoxicity by decreasing phosphorylation of JNK and p38.

Discussion

In the present study, we have demonstrated that rapamycin induces cytotoxicity in MIN6 cells and Wistar rat islets by phosphorylating JNK and p38, and that exendin-4 inhibits this effect by inhibiting phosphorylation of JNK and p38. This is the first report indicating that rapamycin and exendin-4 regulate phosphorylation not only of JNK but also of p38 in primary islets.

The molecular mechanism of the cytoprotective effect of exendin-4 is mediated by increased levels of cAMP that lead to activation of PKA, enhanced IRS-2 activity, and activation of Akt and ERK [7]. Our data also reveal that an increase in the cAMP concentration completely blocked rapamycin-induced cell death. However, LY294002 and PD98059 did not affect rapamycin-induced beta cell death, even though exendin-4 increased Akt and ERK phosphorylation. Phosphorylation of Akt and ERK also were not affected by treatment with rapamycin, suggesting that these kinases are not directly involved in the cytoprotective effect of exendin-4 on rapamycin-induced beta cell death.

On the other hand, exendin-4 and rapamycin both regulate phosphorylation of JNK and p38 in islet beta cells. Rapamycin increases JNK and p38 phosphorylation; exendin-4 decreases their phosphorylation. JNK and p38 are activated by cellular stress, and lead the cells to apoptosis [18]. In islet beta cells, phosphorylation of JNK and p38 are involved in cell death induced by IL-1β [19, 20] and islet isolation [21, 22]. Conversely, inhibition of JNK or p38 with specific inhibitors prevents cell death induced by islet isolation [22, 23], indicating that JNK and p38 are significant molecules in pancreatic beta cell death. In addition, when Wistar rat islets were preincubated for 24 h, rapamycin decreased GSIS, most likely due to reduction in mitochondrial ATP production in the islets of these rats [24]. JNK and p38 are involved in beta-cell function, their activation also affecting insulin biosynthesis. JNK activates c-Jun, a downstream protein, and inhibits insulin gene transcription [25]. Furthermore, the p38 molecule is reported to repress rat insulin gene 1 promoter activated by GLP-1 [26]. Although insulin secretion and insulin content were not affected by pretreatment with 10 nM rapamycin and/or 10 nM exendin-4 for 12 h, inhibition of JNK and p38 activity by treatment with exendin-4 for a longer time may not only inhibit beta cell apoptosis but also increase insulin biosynthesis.

In summary, exendin-4 can inhibit rapamycin-induced beta cell death via a decrease in phosphorylation of both JNK and p38, and dephosphorylation of p38 by exendin-4 is accomplished at least partially through PKA signaling pathways. These results demonstrate that regulation of both JNK and p38 is important in the cytoprotective action of exendin-4 against rapamycin in pancreatic beta cells.

Acknowledgements

This study was supported by Scientific Research Grants from the Ministry of Education, Culture, Sports, Science, and Technology, Japan, and from the Ministry of Health, Labor, and Welfare, Japan, and also by Kyoto University Global COE Program "Center for Frontier Medicine".

Affiliations

[1] Department of Diabetes and Clinical Nutrition, Graduate School of Medicine, Kyoto University, Kyoto, Japan
[2] Japan Association for the Advancement of Medical Equipment, Tokyo, Japan
[3] Department of Endocrinology and Diabetes and Geriatric Medicine, Akita University School of Medicine, Akita, Japan
[4] Kansai Electric Power Hospital, Osaka, Japan
[5] CREST of Japan Science and Technology Cooperation (JST), Kyoto, Japan

References

1 *Kendall DM, Riddle MC, Rosenstock J, Zhuang D, Kim DD, Fineman MS, Baron AD.* Effects of exenatide (exendin-4) on glycemic control over 30 weeks in patients with type 2 diabetes treated with metformin and a sulfonylurea. Diabetes Care 2005; 28: 1083–1091
2 *Baggio LL, Drucker DJ.* Biology of incretins: GLP-1 and GIP. Gastroenterology 2007; 132: 2131–2157
3 *Li L, El-Kholy W, Rhodes CJ, Brubaker PL.* Glucagon-like peptide-1 protects beta cells from cytokine-induced apoptosis and necrosis: role of protein kinase B. Diabetologia 2005; 48: 1339–1349
4 *Yusta B, Baggio LL, Estall JL, Koehler JA, Holland DP, Li H, Pipeleers D, Ling Z, Drucker DJ.* GLP-1 receptor activation improves beta cell function and survival following induction of endoplasmic reticulum stress. Cell Metab 2006; 4: 391–406
5 *Wang Q, Brubaker PL.* Glucagon-like peptide-1 treatment delays the onset of diabetes in 8 week-old db/db mice. Diabetologia 2002; 45: 1263–1273
6 *Li Y, Hansotia T, Yusta B, Ris F, Halban PA, Drucker DJ.* Glucagon-like peptide-1 receptor signaling modulates beta cell apoptosis. J Biol Chem 2003; 278: 471–478
7 *Brubaker PL, Drucker DJ.* Minireview: Glucagon-like peptides regulate cell proliferation and apoptosis in the pancreas, gut, and central nervous system. Endocrinology 2004; 145: 2653–2659
8 *Tews D, Lehr S, Hartwig S, Osmers A, Paslack W, Eckel J.* Anti-apoptotic action of exendin-4 in INS-1 beta cells: comparative protein pattern analysis of isolated mitochondria. Horm Metab Res 2009; 41: 294–301
9 *Bell E, Cao X, Moibi JA, Greene SR, Young R, Trucco M, Gao Z, Matschinsky FM, Deng S, Markman JF, Naji A, Wolf BA.* Rapamycin has a deleterious effect on MIN-6 cells and rat and human islets. Diabetes 2003; 52: 2731–2739
10 *Fraenkel M, Ketzinel-Gilad M, Ariav Y, Pappo O, Karaca M, Castel J, Berthault MF, Magnan C, Cerasi E, Kaiser N, Leibowitz G.* mTOR inhibition by rapamycin prevents beta-cell adaptation to hyperglycemia and exacerbates the metabolic state in type 2 diabetes. Diabetes 2008; 57: 945–957

11 *Fujimoto S, Ishida H, Kato S, Okamoto Y, Tsuji K, Mizuno N, Ueda S, Mukai E, Seino Y.* The novel insulinotropic mechanism of pimobendan: Direct enhancement of the exocytotic process of insulin secretory granules by increased Ca2+ sensitivity in beta-cells. Endocrinology 1998; 139: 1133–1140
12 *Leist M, Gantner F, Bohlinger I, Germann PG, Tiegs G, Wendel A.* Murine hepatocyte apoptosis induced in vitro and in vivo by TNF-alpha requires transcriptional arrest. J Immunol 1994; 153: 1778–1788
13 *Webster AC, Lee VW, Chapman JR, Craig JC.* Target of rapamycin inhibitors (sirolimus and everolimus) for primary immunosuppression of kidney transplant recipients: a systematic review and meta-analysis of randomized trials. Transplantation 2006; 81: 1234–1248
14 *Huang S, Shu L, Dilling MB, Easton J, Harwood FC, Ichijo H, Houghton PJ.* Sustained activation of the JNK cascade and rapamycin-induced apoptosis are suppressed by p53/p21(Cip1). Mol Cell 2003; 11: 1491–1501
15 *Bachar E, Ariav Y, Ketzinel-Gilad M, Cerasi E, Kaiser N, Leibowitz G.* Glucose amplifies fatty acid-induced endoplasmic reticulum stress in pancreatic beta-cells via activation of mTORC1. PLoS One 2009; 4: e4954
16 *Rincón M, Davis RJ.* Regulation of the immune response by stress-activated protein kinases. Immunol Rev 2009; 228: 212–224
17 *Lukowiak B, Vandewalle B, Riachy R, Kerr-Conte J, Gmyr V, Belaich S, Lefebvre J, Pattou F.* Identification and purification of functional human beta-cells by a new specific zinc-fluorescent probe. J Histochem Cytochem 2001; 49: 519–528
18 *Mandrup-Poulsen T.* beta-cell apoptosis: stimuli and signaling. Diabetes 2001; 50 (Suppl 1): S58–S63
19 *Ammendrup A, Maillard A, Nielsen K, Aabenhus Andersen N, Serup P, Dragsbaek Madsen O, Mandrup-Poulsen T, Bonny C.* The c-Jun amino-terminal kinase pathway is preferentially activated by interleukin-1 and controls apoptosis in differentiating pancreatic beta-cells. Diabetes 2000; 49: 1468–1476
20 *Saldeen J, Lee JC, Welsh N.* Role of p38 mitogen-activated protein kinase (p38 MAPK) in cytokine-induced rat islet cell apoptosis. Biochem Pharmacol 2001; 61: 1561–1569
21 *Abdelli S, Ansite J, Roduit R, Borsello T, Matsumoto I, Sawada T, Allaman-Pillet N, Henry H, Beckmann JS, Hering BJ, Bonny C.* Intracellular stress signaling pathways activated during human islet preparation and following acute cytokine exposure. Diabetes 2004; 53: 2815–2823
22 *Ito T, Omori K, Rawson J, Todorov I, Asari S, Kuroda A, Shintaku J, Itakura S, Ferreri K, Kandeel F, Mullen Y.* Improvement of canine islet yield by donor pancreas infusion with a p38MAPK inhibitor. Transplantation 2008; 86: 321–329
23 *Noguchi H, Nakai Y, Matsumoto S, Kawaguchi M, Ueda M, Okitsu T, Iwanaga Y, Yonekawa Y, Nagata H, Minami K, Masui Y, Futaki S, Tanaka K.* Cell permeable peptide of JNK inhibitor prevents islet apoptosis immediately after isolation and improves islet graft function. Am J Transplant 2005; 5: 1848–1855
24 *Shimodahira M, Fujimoto S, Mukai E, Nakamura Y, Nishi Y, Sasaki M, Sato Y, Sato H, Hosokawa M, Nagashima K, Seino Y, Inagaki N.* Rapamycin impairs metabolism-secretion coupling in rat pancreatic islets by suppressing carbohydrate metabolism. J Endocrinol 2010; 204: 37–46
25 *Inagaki N, Maekawa T, Sudo T, Ishii S, Seino Y, Imura H.* c-Jun represses the human insulin promoter activity that depends on multiple cAMP response elements. Proc Natl Acad Sci USA 1992; 89: 1045–1049
26 *Kemp DM, Habener JF.* Insulinotropic hormone glucagon-like peptide 1 (GLP-1) activation of insulin gene promoter inhibited by p38 mitogen-activated protein kinase. Endocrinology 2001; 142: 1179–1187